Capture of CO2 from Steam Reformer Flue Gases Using Monoethanolamine: Pilot Plant Validation and Process Design for Partial

I&EC research
Industrial & Engineering Chemistry Research

pubs.acs.org/IECR

Article

Capture of CO_2 from Steam Reformer Flue Gases Using Monoethanolamine: Pilot Plant Validation and Process Design for Partial Capture

M. Biermann,* F. Normann, F. Johnsson, R. Hoballah, and K. Onarheim

Cite This: *Ind. Eng. Chem. Res.* 2022, 61, 14305−14323

Read Online

ACCESS | Metrics & More | Article Recommendations | Supporting Information

ABSTRACT: Carbon dioxide (CO_2) capture from a slipstream of steam reformer flue gas (18−20 vol $\%_{wet}$ CO_2) using 30 wt % aqueous monoethanolamine was performed for ∼500 h in a mobile test unit (∼120 kg CO_2/h). Specific reboiler duties (SRDs) of 3.6−3.8 MJ/kg CO_2 were achieved at 90% capture. The pilot data validate the modeling of off-design partial capture, that is, operation at lower CO_2 capture rates (at constant gas flow) than the absorption column was designed to achieve. This paper demonstrates that off-design partial capture enables significant energy savings (SRD, cooling) relative to on-design capture. The accrued savings depend on the column design (packing height, flooding approach) and the feed CO_2 concentration. Finally, a concept for stepwise deployment of carbon capture and storage in industries with high-CO_2 concentration sources (e.g., steel and cement manufacturing and refining) is introduced. Thanks to its inherent full-capture-ready design, the initial energy-efficient, off-design partial capture operation can be extended to full capture over time.

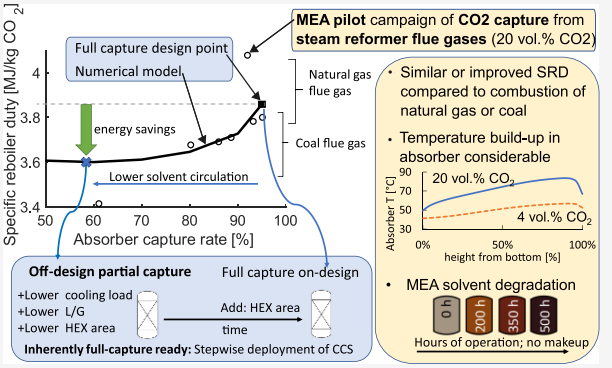

1. INTRODUCTION

Partial capture of CO_2, that is, the capture of only a fraction of the total CO_2 emissions from a stack, is a concept for carbon capture and storage (CCS) that was originally proposed for coal- and gas-fired power plants to meet emission performance standards,[1−3] that is, preceding the requirement for zero or near-zero fossil fuel emissions, to handle flexibility depending on the merit order[4] or to reduce the absolute costs associated with carbon capture.[5,6] In recent years, partial capture has been discussed in terms of a cost-effective near-term mitigation of CCS in process industries, for example, iron and steel, cement, and petroleum refining.[7−11] For these industries, higher flue gas CO_2 concentrations make capture more cost-efficient and an initial CCS deployment more likely.[12] In our previous work,[13] we discussed two fundamental approaches to the design of partial capture from a single CO_2 source: (1) separation of ∼90% of the CO_2 from a slipstream of the gas and (2) separation of ≪90% of the CO_2 from the entire flow of the gas via lower solvent circulation rates. The second approach is preferred in terms of specific reboiler duty (SRD; MJ/kg CO_2 captured), in which the SRD decreases by 12% with a reduction of the capture rate in the absorber from 90 to 45% for a gas with 20 vol % CO_2. So far, however, the modeled savings for SRD at lower capture rates have neither been verified through experiments nor generally characterized as a function of column design and feed gas concentration. Many experimental pilot campaigns[14−28] at relevant scales, that is, representative of scale up to a full-size plant, have been published for low-to-moderate levels of CO_2 concentrations—representative of power plants fired by natural gas (∼3−5 vol % CO_2) or coal (∼12−14 vol % CO_2). Only a few experimental campaigns at a relevant scale that report amine CO_2 capture of gases representative of the CO_2-intensive process industry (more than ∼16 vol % CO_2) have been made publicly available.[29,30]

The present work focuses on partial capture from sources with high CO_2 concentrations, suitable for near-term implementation of CCS, and aims to:

1) Propose a concept for CCS based on off-design partial capture. We define off-design partial capture as partial capture with columns that are designed for full capture (e.g., 95%) and operated at a constant gas flow and lower capture rates (via lower solvent flow rates) in the absorber.

Received: June 21, 2022
Revised: August 20, 2022
Accepted: September 2, 2022
Published: September 16, 2022

Table 1. Overview of MEA Pilot-Scale Campaigns Reported in the Literature[a]

pilot plant	solvent	flue gas	scale (kg_{CO_2}/h)	length (h)	CO_2 conc. ($vol\ \%_{wet}$)	process	pack.height abs./str. (m)	SRD (MJ/kg_{CO_2})	capture rate (%)	comment	ref
C4-NCCC; 2011 baseline	MEA 30 wt %	coal	980	1140	12.1	standard	18/12	3.51	86		14
Korean Pilot	MEA 30 wt %	coal	80	720	15.2	standard	24/17	3.92	90		15
Pilot at Laziska Power Plant	MEA 30 wt %	coal	42	550	11−13	standard	9.2/9.2	3.6−4.0	88−92		21
Tarong CO_2 Capture Pilot	MEA 30 wt %	coal	100	620	10	standard	7.1/7.2	3.6	84		22
Brindisi pilot (ENEL)-40% MEA	MEA 40 wt %	coal	2300	380	11−12 dry	standard	22/11	3.02	89.7	40 wt % MEA	23 24,
Esbjergvaerket Pilot	MEA 30 wt %	coal	1000	2000	n.a.	standard	17/10	3.6−3.7	90		25
MTU at NCCC	MEA 30 wt %	coal	200	500	12.1	standard[b]	18/8	n.a.	n.a.	emissions control	14 26,
RWE Niederaussem Pilot	MEA 30 wt %	lignite coal	300	5000	14.2 dry	standard	n.a.	3.5	90		27
TCM MEA-1	MEA 30 wt %	natural gas	2670	1000	3.4−4.0	standard	24/8	3.8−4.1	90		16 28,
TCM MEA-2	MEA 30 wt %	natural gas	3325	2000	3.6 dry	standard	24/8	3.62	83.4	w/ antifoam	18 19,
TCM MEA-3	MEA 30 wt %	natural gas	3480	2000	4.2	standard	18/8	3.8	87	w/ and w/o antifoam	17
TCM MEA-3 40 wt % MEA	MEA 40 wt %	natural gas	3480	2000	4.2	standard	18/8	3.6	84	w/ antifoam	17
TCM RFCC	MEA 30 wt %	RCCC[c]	8300		13.1−13.5	standard	18/8	3.67	86−89		34
TCM RFCC	MEA 30 wt %	RCCC[c]	8300		13.1−13.5	cold rich by-pass	18/8	3.5	86−89		34
Pilot Kaiserslautern	MEA 30 wt %	synthetic/ gas	∼4	n.a.	5.3	standard	4.25/2.55	3.8	90		33
Pilot Kaiserslautern	MEA 30 wt %	synthetic/ gas	∼8	n.a.	10	standard	4.25/2.55	4.1	90		33
UKCCSRC PACT Pilot	MEA 30 wt %	synthetic/ gas	42		12	standard	6.5/6.1	6.2−6.8	92−95		31 32,
MTU at Brevik-Solvent: S26	ACC's S26	cement kiln	140−150	1600	17.8	standard[b]	18/8	2.8−3.2	∼90	MEA not tested	29

[a]The list is nonexhaustive. [b]Includes proprietary process modifications by Aker Carbon Capture. [c]Residue fluidized catalytic cracker.

https://doi.org/10.1021/acs.iecr.2c02205
Ind. Eng. Chem. Res. 2022, 61, 14305−14323

2) Validate off-design partial capture with large-scale pilot data, specifically by verifying the SRD performance when reducing the capture rate in the absorber, as previously modeled by Biermann et al.[13]
3) Characterize the fundamental qualities and performance of off-design partial capture as a function of column design and CO_2 feed concentration using process modeling.
4) Address the identified gap in the public reporting of monoethanolamine (MEA) data for high CO_2 concentrations. In this work, we report unique measurements of CO_2 capture from steam reformer flue gases (18−20 vol $\%_{wet,CO2}$) using 30 wt % aqueous MEA tested in a mobile test unit by Aker Carbon Capture Norway AS (ACC)[30] for ∼500 h at a relevant scale (up to 126 kg CO_2/h).

This paper is organized as follows. Section 2 briefly reviews the large-scale pilot campaigns using MEA reported in the literature, and this is followed by a short summary of the bulge theory to enable understanding of Section 4. Section 3 describes the setup of the experimental campaign and the method underlying the complementary modeling work. Section 4 presents the experimental and modeling findings separately, before they are discussed together in Section 5.1. The significance of the experimental findings is emphasized in Section 5.2, after which the characteristics of off-design partial capture and its application in the proposed concept are discussed in Section 5.3. The conclusions drawn from this work are presented in Section 6. The Supporting Information provides experimental data and model-derived functions for benchmarking and estimating SRD values as a function of column design.

2. BACKGROUND

2.1. Short Review of Large-Scale Pilot Campaigns on MEA. CO_2 absorption in 30 wt % aqueous MEA has been demonstrated in several large-scale pilot campaigns conducted since 2008. Table 1 gives an overview of the performed MEA campaigns, focusing on steady-state SRD performance. The majority of the pilot campaigns have been conducted on flue gases generated from the combustion of coal (11−13 vol $\%_{wet}$ CO_2) with SRD values mostly in the range of 3.5−3.7 MJ/kg CO_2 for capture rates of ∼90%.[14,15,22,25−27] Some small pilots with <50 kg CO_2/h have reported higher SRD values, closer to 4 MJ/kg CO_2[21] and ≫4 MJ/kg CO_2,[31,32] probably because of insufficient column height. The Technology Center Mongstad (TCM) has supplied the most extensive reports on MEA campaigns. For flue gases derived from the combustion of natural gas (∼4 vol %), Gjernes et al.[17] have described process improvements introduced over three MEA campaigns at 30 wt %, leading to a reduction in SRD from 4.1 MJ/kg CO_2[28] to 3.8 MJ/kg CO_2. Even SRD values of 3.6 MJ/kg CO_2 were reported in the MEA-2 campaign,[18,19] although this value could only be replicated in the later MEA-3 campaign with 40 wt % MEA.[17] Initial findings that showed an improved SRD because the use of an antifoam agent (MEA-2) could not be confirmed in MEA-3.[17] Using a smaller unit, Mangalapally and Hasse[33] have reported similar SRDs for CO_2 concentrations in the range of 5−10 vol %. For flue gases derived from the residue fluidized catalytic cracker (∼13 vol $\%_{wet,CO2}$), which are similar to coal-derived flue gases in terms of CO_2 content, the CO_2 capture at TCM reached an SRD of 3.5−3.67 MJ/kg CO_2 depending on the process configuration.[34] The mobile test unit (MTU) operated by Aker Carbon Capture AS (ACC) has been deployed at various sites for testing different solvents and flue gases, such as those from cement kilns, waste-to-energy plants, and coal-fired and gas-fired power plants (see Askestad et al.[30]). However, most MTU tests have been conducted with ACC's proprietary solvents, and absolute SRD values have not been reported for MEA.[30] Emission levels, but no SRD values, have been reported[14,26] for MEA in the MTU when it was placed at the US National Carbon Capture Center (NCCC).

We have not found any MEA pilot data for CO_2 concentrations above 14−15 vol $\%_{wet}$ CO_2. However, an MTU campaign with one of ACC's proprietary solvents, the S26 solvent, at the cement plant in Brevik, Norway, was reported to have an SRD of 2.8−3.2 MJ/kg CO_2 for cement kiln gases with 17 vol $\%_{wet}$ CO_2.[29]

2.2. Background to the Bulge Theory. Absorbers operate in counter-current mode, that is, a CO_2-lean solvent enters at the top and a CO_2-rich gas enters at the bottom. The descending solvent absorbs CO_2 and heats up due to exothermic absorption enthalpy, causing water to evaporate, which condenses toward the top of column when it comes in contact with the cold solvent.[35] The resulting temperature profile along the column displays a distinct apex or bulge. According to the bulge theory proposed by Kvamsdal and Rochelle,[36] the temperature bulge in the absorber occurs at the highest rate of absorption, which typically occurs away from the pinch, that is, the location in the column where the driving force for absorption between the gas phase and the phase interface equilibrium diminishes to close to zero (mass transfer-limited). Thus, the bulge should occur infrequently at the same position as the pinch and should not overly affect the mass transfer. Depending on the amount of free solvent relative to the feed CO_2, the pinch will occur either: (1) at the top, that is, lean-end pinch (excess solvent) with the highest absorption rate and bulge at the bottom or (2) at the bottom, that is, rich-end pinch (insufficient solvent) with the highest absorption rate and bulge at the top. Impaired mass transfer is, thus, most likely if the pinch and bulge coincide around the middle of the column. Kvamsdal and Rochelle have shown that the maximum bulge temperature occurs at the middle for a specific liquid-to-gas ratio (L/G), that is, the critical L/G at which the absorption enthalpy leaves the absorber in equal shares via the gas and liquid phases. At a lower L/G, the temperature bulge has lesser magnitude and is located closer to the top of the column, and the absorption enthalpy leaves the absorber in higher shares with the gas. At higher L/G values, the temperature bulge is much smaller and appears closer to the bottom of the column, and a greater share of the absorption enthalpy leaves the absorber with the liquid. Finally, Kvamsdal and Rochelle have reported greater magnitudes of the temperature bulge at higher CO_2 concentrations and for more-pronounced changes in the gas-phase CO_2 concentrations (capture rates).

3. METHODS

The methods applied in this work include the experimental campaign with the MTU conducted at a refinery and a numerical model, which is validated with data obtained from the experimental campaign. Section 3.1 describes the setup and equipment of the experimental campaign. Section 3.2 describes the numerical model, its validation, and the conducted modeling study to support and extend the experimental findings.

3.1. Experimental Campaign Using the Mobile Test Unit of Aker Carbon Capture AS. The MTU was installed at Preem's refinery site in Lysekil, Sweden, to demonstrate CO_2

https://doi.org/10.1021/acs.iecr.2c02205
Ind. Eng. Chem. Res. 2022, 61, 14305−14323

capture from the hydrogen production unit, as part of the Preem CCS project.[37] The hydrogen production unit is a steam methane reformer (SMR), which was fed with natural gas and/or butane (in addition to the off-gas from the pressure-swing-adsorption unit). While the CO_2 concentration exiting the SMR varied, it was within the range of 18−20 vol $\%_{wet}$ at the absorber inlet. Both the 30 wt % aqueous MEA and one of ACC's proprietary solvents, the S26 solvent, were tested (results from the S26 campaigns are not presented in this work, while some of the findings are published elsewhere[37]). The MEA campaign was conducted in the period from May 14, 2020, to June 17, 2020, covering a total of 508 h of operation and 52.4 tons of CO_2 captured. The measured flue gas characteristics for the MEA campaign are listed in Table 2.

Table 2. Flue Gas Characteristics Measured throughout the Campaign [Mean Value, Minimum Value, Maximum Value, and Standard Deviation (STD) of the Mean]

parameter (sampling site)	unit	mean value	min./max./STD
temperature (stack)	°C	160	152/168/3.32
O_2 (stack)	vol%	4.44	3.51/5.90/0.44
CO (stack)	ppmv	1.60	0.39/3.64/0.74
NO (stack)	ppmv	34.0	27.2/41.8/4.96
NO_2 (stack)	ppmv	1.78	1.53/2.11/0.11
SO_2 (stack)	ppmv	0.91	0.16/1.69/0.45
temperature (absorber inlet)	°C	34.1	30.7/49.9/4.99
flow (absorber inlet)	Sm^3/h	349.3	285/414/19.5
CO_2 (absorber inlet)	vol%	18.7	17.6/20.3/0.71
H_2O (absorber inlet)	vol%	5.10	4.04/11.4/1.63

Figure 1 shows a simplified flowsheet of the ACC capture process. This standard postcombustion solvent process is the design basis for MTU. Proprietary process solutions regarding energy efficiency and emissions control are confidential and are not included in the flowsheet. For graphical illustrations of the MTU, see refs 26, 30, 38. Table 3 shows the MTU design data. The capacity of the MTU is up to 150 kg CO_2/h with absorber/desorber packing heights that are representative of a full-scale plant. The MTU uses an electrical reboiler, which allows for accurate measurements of the consumed reboiler energy. However, because of the relatively small size of the MTU

Table 3. Design Data of the MTU Operated by Aker Carbon Capture[a]

parameter	unit	value
maximum gas flow	Sm^3/h	1000
CO_2 capture efficiency	%	~90
absorber diameter	m	0.40
absorber packing height	m	11−18
desorber diameter	m	0.32
desorber packing height	m	8
solvent circulation rate	m^3/h	0−3.6

[a]Adopted from refs 29, 39.

compared to full-scale units, heat losses have a non-negligible effect on the SRD. The heat losses from major items based on actual dimensions of insulated and noninsulated equipment were estimated as 4.5−5.5 kW considering the hourly averaged local ambient temperature and wind speeds for each test run obtained from the nearest weather station to Lysekil (Måseskär, Väderöarna). These losses accounted for 4−6% of the measured power consumption. All the experimental SRD values reported in this work have been corrected for heat losses. An online emissions analyzer monitors CO_2 capture and emissions online. It measures continuously the gas alternating between the absorber inlet (downstream of the DCC), absorber outlet (downstream of the washer section), and desorber outlet via connected heated sampling lines (180 °C). The emission analyzer is calibrated for a list of standard flue gas pollutants, for example, CO, CO_2, SO_2, HCl, NO, NO_2, NH_3, as well as MEA, and H_2O. The detection limit of the emission analyzer system is approximately 1 ppmv. The CO_2 mass balance was checked by comparing the absorber balance of the ingoing and outgoing CO_2 with the CO_2 flow measured downstream of the stripper. Both approaches were in good agreement and the deviation from their mean value within ±5% (see Figures S.1a and S.1b in the Supporting Information). The measurement made at the stripper gas side is considered more reliable because of the straightforward measurement principle applied (orifice with dP measurement downstream of the condenser, accounting for the temperature-derived saturation of CO_2 with water), whereas the absorber gas-based measurement depends on both the gas flow measurement and the emission analyzer values for the CO_2

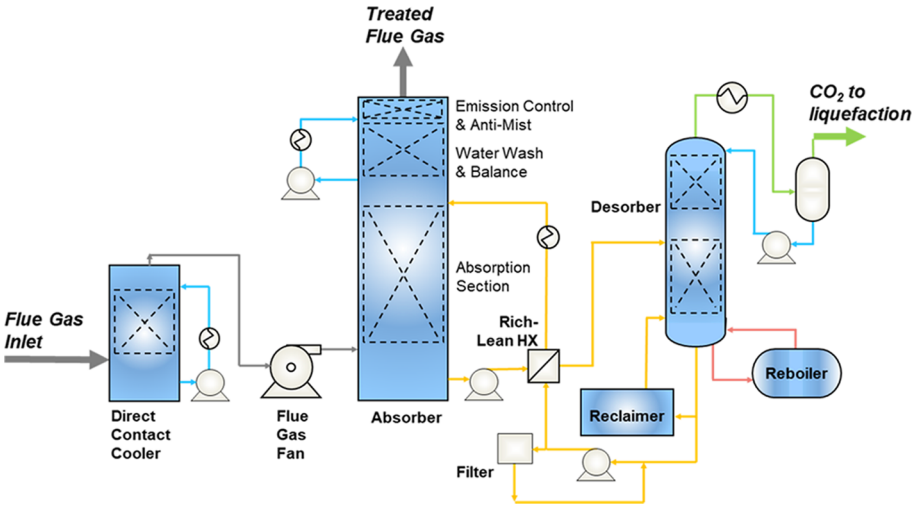

Figure 1. Simplified generic flowsheet of the ACC capture process. From ref 37.

https://doi.org/10.1021/acs.iecr.2c02205
Ind. Eng. Chem. Res. 2022, 61, 14305−14323

Table 4. Tested Parameters in the MEA Campaign Conducted in the MTU[a]

tested parameter	range	varied	targeted
reboiler temperature (°C) (lean loading); "u-curve"	117−121	reboiler duty; solvent flow rate	separation rate of 90%
flue gas temperature (°C) (absorber inlet)	30−50	DCC outlet temperature; solvent flowrate	separation rate of 90%; reboiler temperature[b]
separation rate (absorber)	60−90%	solvent flowrate	separation rate as specified; reboiler temperature[b]
absorber packing height (m); constant gas flow	11, 18	packing section; solvent flow rate	separation rate of 90%; reboiler temperature[b]
absorber packing height (m); constant L/G	11, 18	packing section; gas and solvent flow rates	separation rate of 90%; reboiler temperature[b]
stripper pressure (bara)	1.5, 1.9, 2.5	stripper bottom pressure	separation rate of 90%; rich and lean CO_2 loadings maintained

[a]L/G, liquid-to-gas ratio. [b]The temperature (lean loading) that gave the lowest SRD from the reboiler temperature test was chosen for the remaining runs.

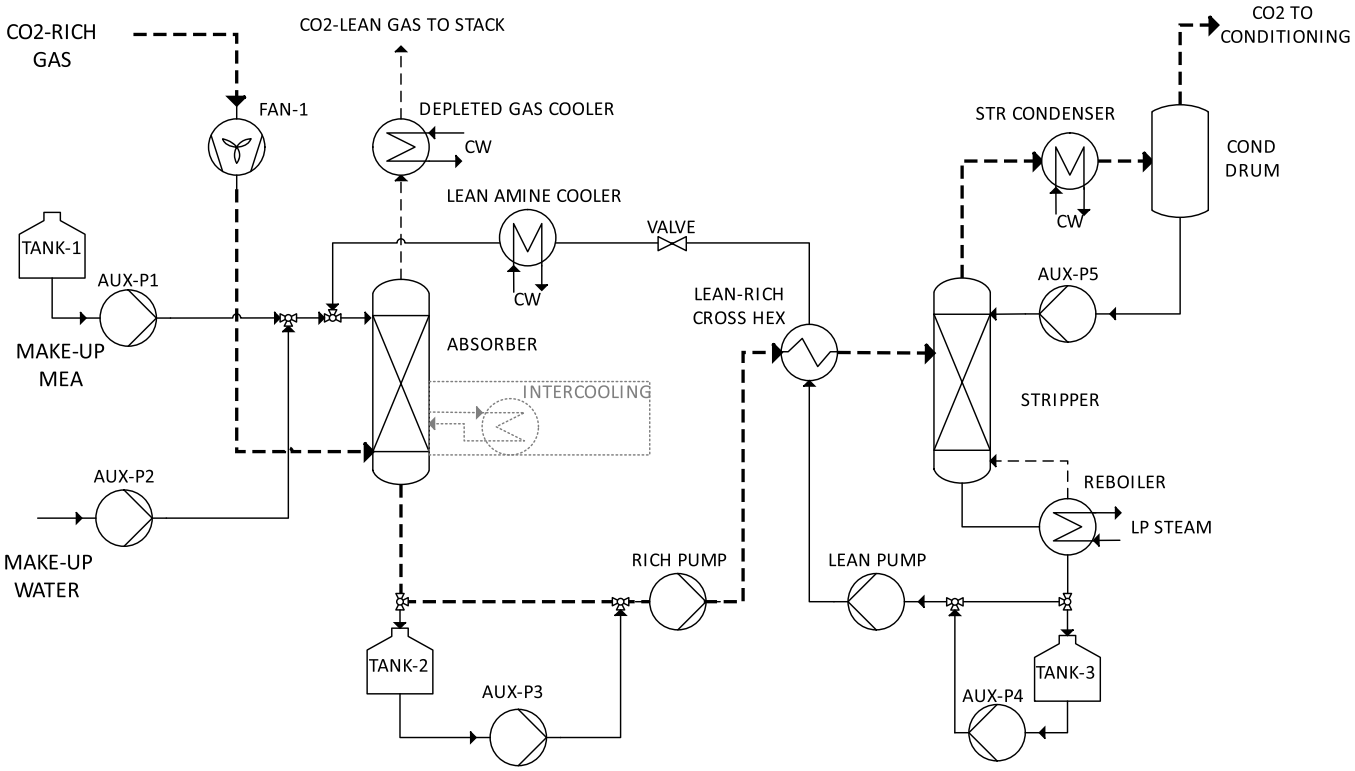

Figure 2. Flowsheet of the standard amine-based capture process. The flowsheet is simplified in that a direct-contact cooler and the washer section are excluded from the modeling. The intercooling modification is shown in gray, dashed lines and was not active as per default.

concentrations of the ingoing and outgoing gases. Thus, all quantities related to CO_2 were based on the stripper gas-side flow rate. For most of the campaigns, a capture rate of 90% was targeted and achieved; the active variation of the parameter resulted in a span of 60−95% (see Figure S.1c in the Supporting Information). Note that only up to 126 kg CO_2/h of captured CO_2 were reached because of restrictions imposed on the gas flow by the high CO_2 concentrations.

The campaign investigated the impacts of the following five parameters on the SRD: reboiler temperature (lean loading); absorber separation rate; flue gas inlet temperature; absorber packing height; and stripper pressure. Table 4 gives an overview of the tested ranges and controlled parameters. For each run, that is, tested parameter value, the measurements recorded over 2 h of stable, steady-state operation were averaged. It should be noted that no MEA makeup was added. Samples of the CO_2-lean/-rich solvents were taken at the end of each run (alkalinity, density) and samples for external analyses of solvent parameters were collected regularly. Only the solvent sample at the very end of the campaign (dated June 17; see Table S.1 in the Supporting Information) could be analyzed in detail, as the remaining samples were lost in the mail.

3.2. Numerical Model. *3.2.1. Model Description.* The modeling was carried out in the Aspen Plus V12 software (Aspen Technology Inc., Bedford, MA, USA). The solvent used was an aqueous solution of 25−30 wt % MEA. The model is based on previous work[13,40] and has been revised regarding the property method and reaction sets based on the Aspen Plus model developed by AspenTech.[41] The liquid properties were estimated by the ENRTL-RK method, and the vapor phase equation-of-state was Redlich-Kwong. All the columns were modeled using rate-based calculations. Furthermore, in all the columns, a counter-current flow of vapor and liquid was applied. Mass transfer coefficients and interfacial areas in the packings were predicted using the 1985 correlations described by Bravo et al.[42] The liquid holdup was calculated with the 1989 Stichlmair

https://doi.org/10.1021/acs.iecr.2c02205
Ind. Eng. Chem. Res. 2022, 61, 14305−14323

Table 5. Model Parameters (Rate-Based Settings and Other Column-Related Settings) Chosen after Comparison with Data from the Experimental MEA Campaign in this Work

rate-based parameters	value/setting	comment
mass transfer/interfacial area	Bravo, Rich, Fair 1985 (BRF 85)	others tested: BRF 92 (large deviation); Hanley-Struc2010 (more similar to BRF 85)
holdup method	Stichlmair 1989	others tested: BRF 92 (similar to Stichlmair, slightly higher SRD)
flow model	VPlug	41
interfacial area factor	0.8	others tested: 0.8−1.2; default value of 1 shows slightly larger deviation from exp. temperatures
reaction condition factor	0.9	41
film discretization ratio	5	41
other parameters		
packing type	Koch Glitsch: FLEXIPAC 2X	
pressure drop method	Wallis	41
stages (absorber/stripper)	30/20	
vapor phase equation-of-state	Redlich-Kwong	others tested: PC-SAFT (similar performance, slightly higher SRD and slightly lower reboiler temperature)

correlation.[43] Heat transfer coefficients were obtained via the Chilton and Colburn analogy.[44] The reactions occurring in the absorber and in the stripper were set up following the work of Zhang and Chen,[45] who included the kinetic parameters derived by Pinsent et al.[46] and Hikita et al.[47] Figure 2 shows the standard capture process configuration. It should be noted that no direct-contact cooler or washer section was included in the model for the sake of simplicity and to ease convergence. The depleted gas cooler shown instead for the washer was included to facilitate the comparability of model runs with regard to cooling loads. Furthermore, the process modification using intercooling was only active for one subcase (see Section 3.2.3).

To describe and evaluate the numerical work, the following definitions are applied:

- Column design encompasses the geometric column specifications, specifically the packing height and the packing diameter determined via the design factor (also called the approach to flooding or fraction of flooding).
- Design point or on-design operation is the operational point in a given column design which corresponds to a capture rate of 95% at the lowest SRD value found through variation of the lean loading and solvent circulation.
- Off-design partial capture represents the operation at capture rates below the design point (fixed column geometry).
- Minimum SRD (SRD_{min}) is the capture rate at which the lowest SRD value is observed when operating in off-design mode.

The design factor, *DF*, is defined as the ratio of the gas capacity factor F in the column to the gas capacity factor at flooding F_{flood} (see eq 1). The gas capacity factor F is the maximum gas capacity in the column at the operating point. When operating in on-design mode, the theoretical stage at which the gas capacity factor F is observed is called the "design stage" (see eq 1). The column diameter was calculated according to eq 3, as described previously.[48] Equations 1−3, including the determination of the flood point (and thus F_{flood}) via the pressure drop correlation (see Table 4), are implemented in Aspen Plus by default. Other column characteristics, that is, the absorber liquid residence time, liquid to gas ratio (L/G), and the specific packing volume were calculated according to eq 4, eq 5, and eq 6 and eq 7, respectively. Key performance indicators for energy consumption, that is, SRD, specific cooling demand (SCD), specific power demand (SPD), and deviations from minimum SRD when varying the capture rate ($Dev_{SRD_{min}}$ and $Dev_{SRD_{min},\ design\ 95\%}$), were calculated according to eqs 8−12 (for an explanation of abbreviations, see the Notation section).

$$DF = F/F_{flood} \times 100\ [\%] \tag{1}$$

$$F = u_{gas,design\ stage} \times \sqrt{\rho_{gas,design\ stage}}\ [\sqrt{Pa}] \tag{2}$$

$$d = \sqrt{\frac{4}{\pi}} \cdot \sqrt{\frac{\dot{m}_{gas,design\ stage}}{\sqrt{\rho_{gas,design\ stage}} \cdot F}}\ [m] \tag{3}$$

$$\tau_{liq,abs} = \frac{V_{holdup}}{\dot{V}_{lean\ solv,abs}}\ [min] \tag{4}$$

$$\frac{L}{G} = \frac{\dot{m}_{lean\ solv,abs}}{\dot{m}_{gas,abs}}\ [Kg/Kg] \tag{5}$$

$$V_{packing} = h \cdot \frac{\pi d^2}{4}\ [m^3] \tag{6}$$

$$V_{packing,spec.} = \frac{V_{packing,abs} + V_{packing,str}}{\dot{m}_{CO_2,captured}} \left[\frac{m^3}{t\ CO_2/h}\right] \tag{7}$$

$$SRD = \frac{\dot{Q}_{reb}}{\dot{m}_{CO_2,captured}} \left[\frac{MJ}{kg\ CO_2}\right] \tag{8}$$

$$Dev_{SRD_{min}} = \frac{SRD - SRD_{min}}{SRD_{min}} \times 100\ [\%] \tag{9}$$

$$Dev_{SRD_{min},design\ 95\%} = \frac{SRD - SRD_{min}}{SRD_{design,95\%} - SRD_{min}} \times 100\ [\%] \tag{10}$$

$$SCD = \frac{\dot{Q}_{cool}}{\dot{m}_{CO_2,captured}} \left[\frac{MJ}{kg\ CO_2}\right] \tag{11}$$

$$SPD = \frac{P_{rotary}}{\dot{m}_{CO_2,captured}} \left[\frac{MJ}{kg\ CO_2}\right] \tag{12}$$

3.2.2. Model Verification. The verification of the model performance through data from the experimental campaign was performed in off-design mode, that is, the column geometry was set to the column geometry of the MTU, as described in Table 3.

https://doi.org/10.1021/acs.iecr.2c02205
Ind. Eng. Chem. Res. 2022, 61, 14305−14323

Note that as the MTU does not have a lean amine cooler, the unit was excluded from the model used for the verification. The model process parameters (column inlet temperatures, pressures, gas flow, etc.) were set to resemble the experimental test runs that provided the lowest SRD values in the u-curve trials (because these runs were the most-repeated throughout the campaign) (see Table S.3 in the Supporting Information). In addition, the MEA content was set to 25 wt %, to represent the loss of MEA throughout the campaign (see Section 4.1.4). To confirm the validity of the original model settings[41] and possibly improve the match with the measured absorber temperature profiles, various parameters in the setup for the rate-based calculations were varied first individually, in the order of observed, decreasing impact on the absorber temperature profiles, and then in combination. The parameters include combinations of mass-transfer correlation and holdup correlation (similar to the ones in ref 41), as well as the packing type and interfacial area (because information on the exact packing specification as implemented in the MTU is confidential and was nondisclosed in the modeling work), and the reaction conditioning factor, that is, a weighting factor between 0 and1 (factor × bulk condition + (1 − factor) × interface) for the calculation of reaction rates. A higher factor implies liquid conditions closer to the bulk liquid will have a higher weight.[49] However, the reaction conditioning factor showed little impact on the temperature profiles. The parameters finally chosen (Table 5), that is, which provided the best fit in temperature profile, are similar to the original model settings.[41] The measured profiles taken from the campaign in this work for a mean capture rate of 89.6% (range, 88.6−90.6%) and the simulated absorber temperature profile for 90% capture are shown in Figure 3. The experimental and modeled profiles, as

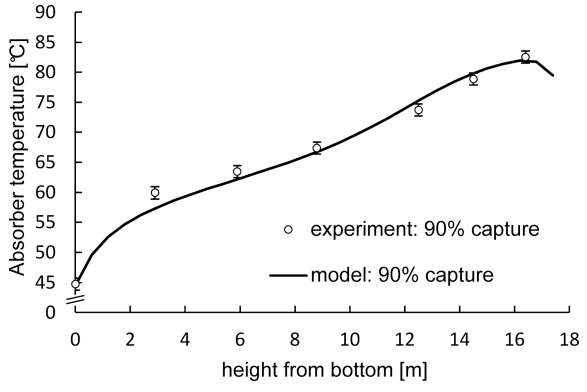

Figure 3. Model verification with temperature profiles. Shown is a comparison of the found model settings for a capture rate of 90% and the experimental values from the MEA campaign in this work, showing a mean of 89.6% capture (range, 88.6−90.6%) for the included test points (lowest SRD value at ∼120 °C from the u-curve trials). Note that the ordinate is truncated.

well as the bulge locations and magnitudes, show a good match. The u-curve comparing the experimental (mean, 89%; range, 85−91% capture) and modeled SRD (89% capture) for different reboiler temperatures is shown in Figure 4. The reader is directed to Table S.2 in the Supporting Information for the experimental u-curve data. The model follows the trend of the experimental values, and the lowest SRD is at a similar location of ∼120 °C, which corresponds to a lean loading of 0.17 mol CO_2/mol MEA in both the experimental and modeling situations (see Table S.3 in the Supporting Information). The

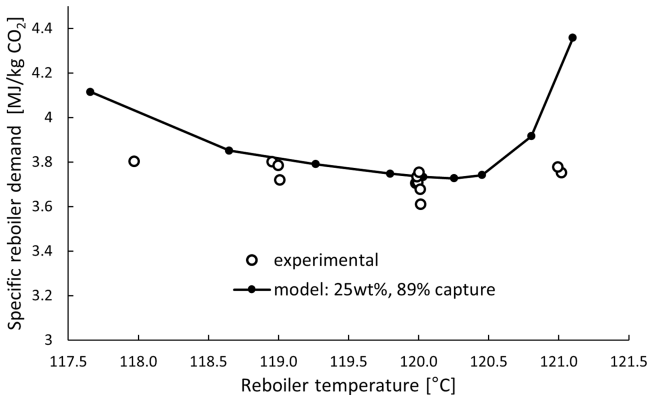

Figure 4. u-Curve generated with the model at a capture rate of 89% using the rate-based settings in Table 5, as compared with the experimental u-curve obtained from the MEA campaign in this work (mean capture rate, 89%; range, 85−91%). See Table S.3 Supporting Information for the comparison of the modeled and experimental results obtained at 120 °C, and Table S.2 Supporting Information for the experimental u-curve data.

deviation toward the experimental values is greater at the edges of the temperature span. In general, the modeling yields slightly higher SRD values than the experiments.

3.2.3. Column Design and Intercooling Study. A design study quantifies the impacts of CO_2 concentration and column design on the energy performance of off-design partial capture. In this study, the absorber packing height, the CO_2 concentration (wet, saturated with H_2O at 40 °C), and the design factor for both the stripper and absorber column were varied, while the remaining process parameters were kept constant as shown in Table 6. The setup of the design study was adjusted to comply with common assumptions/process parameters (including an amine cooler) and used the rate-based settings derived from the model verification (see Table 5). The modeling approach is described by the following steps:

1. The flue gas was specified according to the chosen CO_2 concentration and water saturation level (nitrogen was used to model the remainder of the gas).
2. The column design (absorber packing height, design factor for absorber and stripper) was specified, and the design mode used to calculate the diameter was activated in Aspen Plus. Note that the stripper height was fixed (having a significantly weaker impact than the absorber height).
3. The lean loading and the solvent circulation rate were varied (u-curve approach), so as to identify the lowest SRD value for a capture rate of 95%, which was considered the design capture rate.
4. The column hydraulics in Aspen Plus were checked to ensure that the maximum gas capacity occurs at the design stage [see eq 2], such that the calculated column diameter is representative. The design stage in the absorber was found in the top quarter of the packing, while the design stage in the stripper was found in the bottom stage in all cases.
5. Once the design point was determined (steps 1−4), the column geometry was fixed (the design mode to calculate the diameter was deactivated), so as to model off-design partial capture. Thus, the capture rate was lowered stepwise (10 percentage points) to 50% by varying the solvent flow rate whilst maintaining the lean loading.

https://doi.org/10.1021/acs.iecr.2c02205
Ind. Eng. Chem. Res. 2022, 61, 14305−14323

Table 6. Varied and Constant Process Parameters Used in the Design Study

parameter	unit	value	comment/reference
varied parameters			
absorber packing height	m	15, 20, 25	
design factor (flooding approach)	%	60, 70, 80	common design range: 60–80%[48,50,51]
CO_2 concentration	vol%$_{wet}$	4, 10, 20	
constant parameters			
flue gas flow	kmol/h	15,615	~350 kN m^3/h
lean MEA concentration in water	wt %	30	
stripper packing height	m	10	
cross-heat exchanger ΔT (hot outlet/cold inlet)	°C	10	
lean solvent absorber inlet T	°C	40	lean amine cooler assumed
gas absorber inlet T	°C	40	
depleted gas discharge T	°C	40	set to a constant temperature to allow comparable cooling demands
column pressure drop	bar	0.05	order of magnitude of packing pressure drop
stripper top gas condenser	°C	30	
stripper pressure	bara	1.9	
flue gas fan pressure increase	bar	0.1	
rich solvent pump pressure increase	bar	3	
rotary equipment isentropic efficiency	%	85	
rotary equipment mechanical efficiency	%	95	

While capture rates of <50% are possible in principle, they were omitted because previous work showed that the SRD increases at capture rates below approximately 50%.[13] Moreover, the operational performances of some items of equipment (pumps, columns) may be constrained at capture rates of <50% (see Section 5.3).

In addition to the design study, intercooling of the absorber was studied, to quantify the impact of active temperature management in the absorber column at high CO_2 concentrations (20 vol %). The SRD values of the following four cases were compared:

- DA—adiabatic on-design, that is, capturing 95% of the CO_2 with a column design with 20 m of absorber packing and a design factor of 80%.
- DSC—on-design with single-stage intercooling (same design point as DA). The intercooling stage was modeled as pump-around (return stage immediately below the draw stage). The intercooling location (return and draw stages) was varied to identify the location with the lowest SRD.
- DMC—on-design with multistage intercooling (same design point as DA). The intercooling was modeled as simple column coolers with an evenly distributed cooling load at stages 5, 10, 15, 22, and 27 (of 30 stages in total).
- OFFD—adiabatic off-design partial capture close to the minimum SRD (same design point as DA).

4. RESULTS

The results are presented in two sections. The first section focuses on the experimental findings and the second section on the results of the modeling. The relationships between the experimental and modeling results are discussed in Section 5.1.

4.1. Experimental MEA Campaign. This section includes the experimental findings regarding energy performance, emissions levels, and solvent degradation. The results related to stripper pressure and lower column height at constant L/G are given in the Supporting Information in Figures S.3 and S.4, respectively.

4.1.1. U-Curves of Reboiler Duty versus Temperature. Figure 5 shows the so-called "u-curve," representing the SRD versus the reboiler temperature (or lean loading), for the present

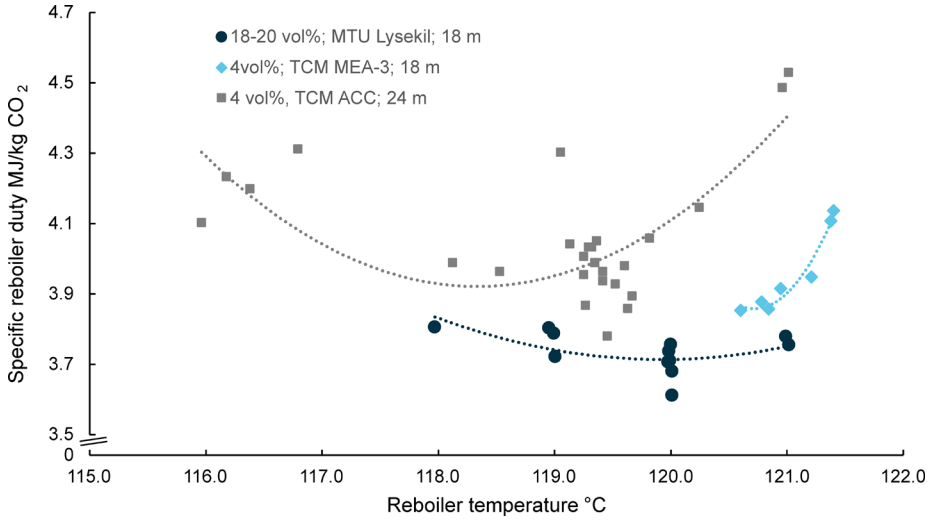

Figure 5. SRD versus reboiler temperature (u-curves), with measurements from the MTU pilot obtained in the Preem CCS campaign (this work, circles) compared to the results of the MEA-3 campaign at TCM with the same packing height of 18 m (diamonds) reported by Gjernes et al.,[17] as well as to the results of the MEA campaign conducted by ACC at TCM with a packing height of 24 m (squares) reported by Gorset et al.[16] The depicted, second-order polynomial fitted curves indicate the shapes of the obtained u-curves. Note that the ordinate is truncated.

https://doi.org/10.1021/acs.iecr.2c02205
Ind. Eng. Chem. Res. 2022, 61, 14305−14323

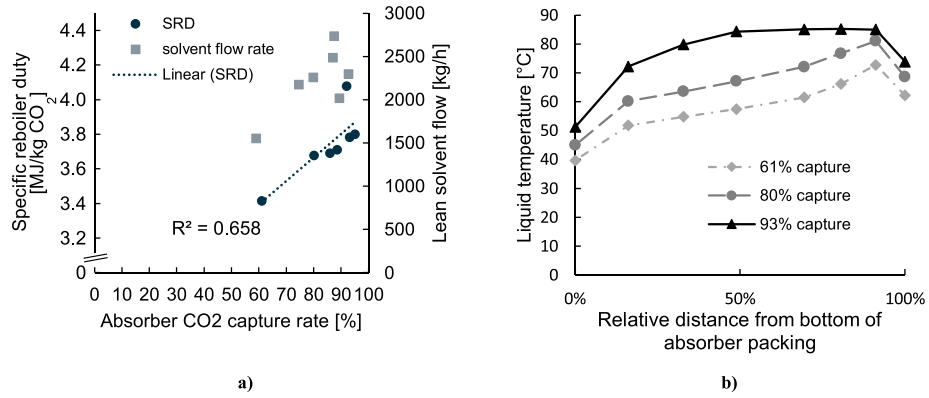

Figure 6. SRD versus absorber capture rate at 18−20 vol $\%_{wet}$ CO_2 (a) and characteristic absorber liquid temperature profiles (b) for 350 Sm^3/h, with 20 vol $\%_{wet}$ CO_2 depending on the capture rate obtained by variation of the solvent flow. Note that the ordinate in (a) is truncated.

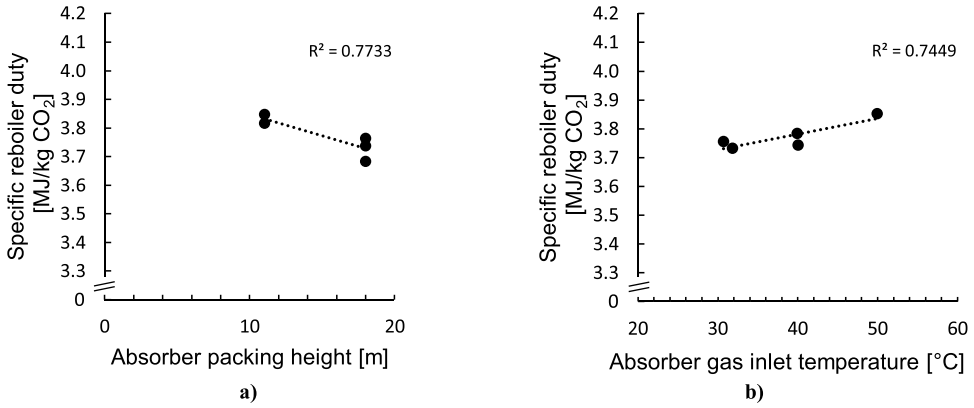

Figure 7. Effects of packing height (a) and flue gas temperature (b) on the SRD. Note that the ordinates are truncated.

campaign, and relates it to comparable measurements from the literature. The SRD range measured with the MTU for the SMR flue gas (18−20 vol $\%_{wet}$ CO_2) was 3.6−3.8 MJ/kg CO_2 for a capture rate of ∼90%. A minimum SRD is seen at 120 °C, with the lowest measured SRD at 90% capture of 3.61 MJ/kg CO_2 (one run) yet on average 3.70 MJ/kg CO_2 (6 runs). As expected, the measured SRD range was lower than the pilot campaign with MEA at TCM,[16,17] where CO_2 was captured from a gas-fired CHP plant with CO_2 concentrations of ∼4 vol $\%_{wet}$. The 30 wt % MEA campaign at TCM conducted by ACC in 2014 used the full height of 24 m, targeted capture rates of 80−90%,[16] and achieved SRD values of 3.8−4.5 MJ/kg CO_2 (outliers of up to 6 MJ/kg CO_2, not shown) with a minimum SRD closer to 119 °C. The more recent MEA-3 campaign (2018) at TCM has achieved 3.8−4.1 MJ/kg CO_2 with a packing height of 18 m (same height as the MTU), with the minimum closer to 121 °C.[17] The MTU u-curve of the present work appears flatter than the TCM curve,[16] which may have various reasons not only related to the CO_2 concentration, such as process layout or operating point in respect to design. Finally, it should be noted that the measured SRD is at the upper end of the reported range for coal-based flue gases (3.5−3.7 MJ/kg CO_2) (see Table 1). The u-curve data are provided in the Supporting Information in Table S.2.

4.1.2. Partial Capture and Temperature Profiles. The measured effect of the capture rate in the absorber on the SRD is shown in Figure 6a, together with the observed liquid temperature profiles in the absorber (right panel). The SRD of ∼3.7 MJ/kg CO_2 at ∼90% capture decreased when the capture rate was lowered via a reduction in solvent flow rate. The lowest measured value of ∼3.4 MJ/kg CO_2 was found at a capture rate of ∼60%. Figure 6b reveals that the absorber temperature levels are lower at lower capture rates. The bulge temperature decreased from ∼85 to ∼73 °C when the capture rate was reduced from ∼90 to ∼60%. The maximum temperature (bulge) was measured at the same location. Note that the spread of the measured SRD values is relatively large—a linear fit gave an R^2 value <0.7—preventing a meaningful mathematical fit with power law or exponential functions that would describe the expected exponential increase in SRD with higher capture rates.

4.1.3. Process Parameters: Impacts of Gas Temperature and Packing Height on the SRD. Figure 7 shows the impacts of absorber packing height (at constant gas flow) and flue gas temperature at the absorber inlet on the SRD. Decreasing the packing height from 18 to 11 m resulted in a relative increase in the SRD of ∼0.1 MJ/kg CO_2. An increase in the SRD of similar magnitude was observed when increasing the flue gas temperature entering the absorber from 30 to 50 °C (0.005 MJ/kg CO_2 per 1 °C).

4.1.4. Emissions and Solvent Degradation. The MEA solvent underwent considerable degradation during the 500-h campaign, as evidenced by the discoloring of the solvent (see Figure S.2 in the Supporting Information), the measured levels of degradation compounds (acids, heat stable salts, and organic compounds) in the solvent at the end of the campaign (see Table S.1 in the Supporting Information), and the levels of ammonia emissions in the CO_2-depleted absorber top gas. Figure 8 shows the measured levels of ammonia emissions (ppmv) in the CO_2-depleted flue gas, revealing an increasing trend over time, as well as higher levels compared to previous campaigns with lower CO_2 concentrations.[16,52] The levels of

https://doi.org/10.1021/acs.iecr.2c02205
Ind. Eng. Chem. Res. 2022, 61, 14305−14323

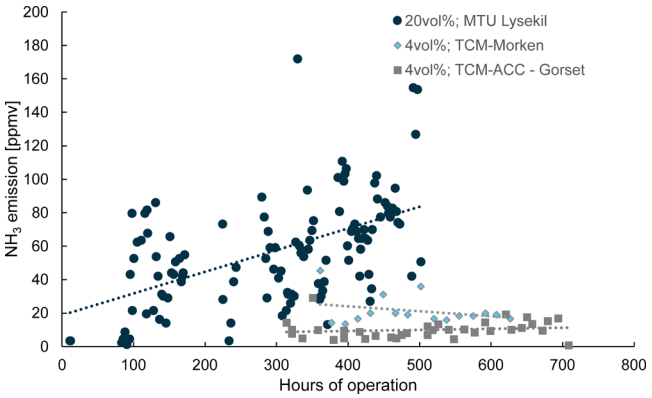

Figure 8. Levels of ammonia emissions in the CO_2-depleted absorber top gas (downstream of the washer section). Results from the MTU campaign (this work, circles) compared to the results from the MEA TCM campaigns as reported by Gorset et al.[16] and Kolstad Morken et al.[52]

MEA emissions to air were low, mostly below the detection limit of the emissions analyzer (<1 ppmv). Overall, the MEA solvent loss during the 500-h campaign was estimated as 1.1 kg/t CO_2 captured. Because no solvent makeup was added, the initial alkalinity of 4.8 mol/kg solvent (~29 wt % MEA in H_2O) decreased to 3.8 mol/kg solvent (~23 wt % MEA in H_2O) at the end of the campaign.

4.2. Modeling Results. *4.2.1. Absorber Characteristics for High CO_2 Concentrations when Varying the Capture Rate.* Figure 9 shows the SRD for a CO_2-rich gas with 20 vol %$_{wet}$ CO_2

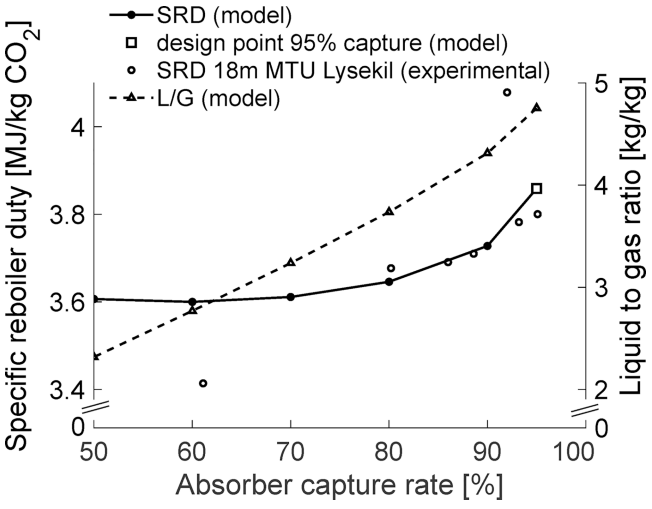

Figure 9. SRD and liquid-to-gas ratio (L/G) versus absorber CO_2 capture rate for 20 vol %$_{wet}$ CO_2 for a fixed column design with 95% capture, packing height of 20 m, and design factor of 80%. The experimental values from Figure 6 are included for comparison (packing height of 18 m, 18−20 vol % CO_2). Note that the ordinates are truncated.

as a function of the achieved capture rate for a fixed column design at 95% capture and with a design factor of 80%. The experimental results (cf. Figure 5) are shown for comparison (18−20 vol %$_{wet}$ CO_2). The model response showing increasing SRD in line with increasing capture rate is in agreement with the experimental findings. Most of the measurements are close to the modeled curve, although some considerable deviations are observed. The model found a minimum SRD of 3.6 MJ/kg CO_2 at a capture rate of ~60%, from which the design point SRD (95% capture) deviates by 7%. In comparison, the experiments found a larger deviation of 8−11% (outlier of 19%) for 90% capture from the minimum SRD (3.4 MJ/kg CO_2). Approximately half of that deviation from the minimum SRD in the model occurs between 60 and 90% capture, with the other half occurring at >90% capture. The liquid-to-gas (L/G) ratio increases linearly with the capture rate (being slightly higher at capture rates above 90%).

Figure 10 illustrates how the absorber profiles for liquid temperature, CO_2 loading, and driving force change with the

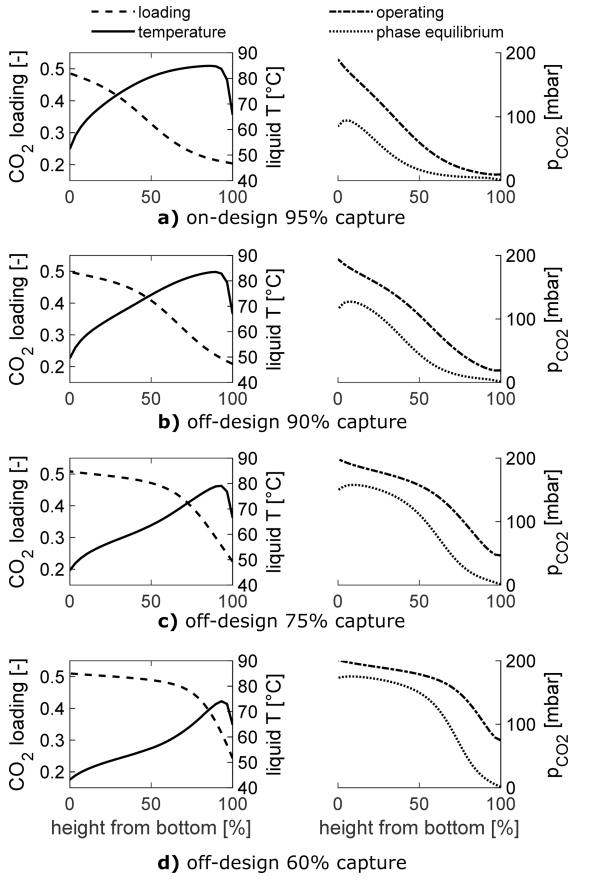

Figure 10. Absorber profiles for liquid temperature and molar CO_2 loading (left panels) and McCabe-Thiele plots of the partial CO_2 pressure (right panels) depending on the capture rate (rows a−d) for a fixed absorber design (height of 20 m, design factor of 80 and 95% capture) and a CO_2 concentration of 20 vol %$_{wet}$. Plots are obtained from the model simulations performed in this work.

capture rate, as obtained from the model simulations in this work. For high capture rates (high L/G ratios), a so-called "lean-end pinch" in the absorber is observed (the same observation is made for 4 and 10 vol %$_{wet}$ CO_2) (see Figures S.5 and S.6 in the Supporting Information). The high capture rate gives a relatively low partial pressure of CO_2 in the gas leaving the column. Consequently, CO_2 absorption occurs at lower rates in the upper section of the column. High liquid temperatures are observed, which are caused by increased reaction rates at the high CO_2 concentrations (lower temperatures are seen for 4 and 10 vol % CO_2 in Figures S.5 and S.6 in the Supporting Information, respectively). The bulge temperature is 85 °C and the bulge is located near the top of the column; similar to what is seen in the experiments (cf. Figure 6). For lower capture rates

https://doi.org/10.1021/acs.iecr.2c02205
Ind. Eng. Chem. Res. 2022, 61, 14305−14323

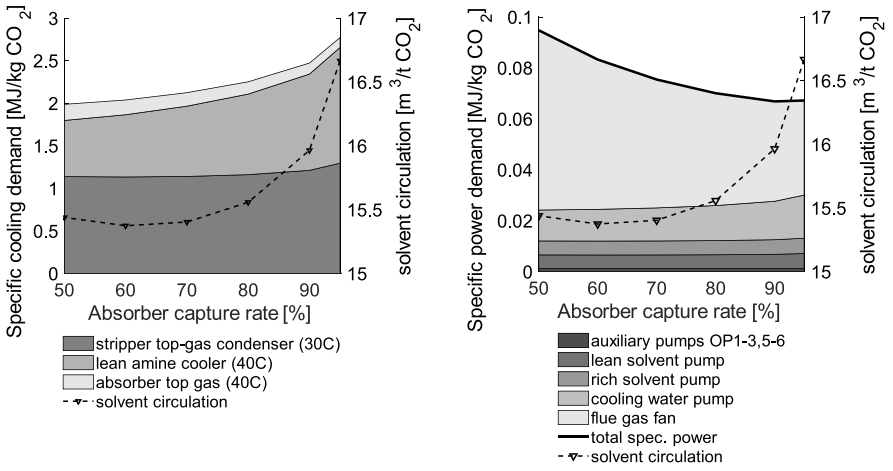

a) b)

Figure 11. SCDs with cooler contributions (a) and SPD with rotary equipment contributions (b), as obtained from the modeling in this work. Modeling is performed for a CO_2 concentration of 20 vol $\%_{wet}$ at a fixed column design of 95% capture, packing height of 20 m, and design factor of 80%. Note that neither the direct contact cooler nor the CO_2 conditioning is included here (cf. Figure 2).

(Figure 10b–d), less reaction heat is developed, and the absorber exhibits lower liquid temperatures. The bulge temperature decreases, and its location is pushed upward with decreasing L/G ratios, which is in line with the documented bulge theory of Kvamsdal and Rochelle.[36] The rate of uptake of CO_2 into the liquid phase in the upper section of the column is increased (steeper gradient), such that the solvent becomes saturated after a shorter contact time, because less solvent is available to capture CO_2 (the solvent saturation front is shifted upward) as compared to the higher L/G ratios. Toward the bottom of the column, the driving forces diminish (a tendency toward a rich-end pinch can be seen). Overall, the achieved higher rich loading of 0.51 at the capture rate of 60% leads to a lower SRD in the stripper column, as compared to a rich loading of 0.49 at 95% capture (on-design).

Figure 11a shows the specific cooling, and Figure 11b shows the power demand per kg of captured CO_2 as a function of the absorber capture rate, as obtained from the model simulations of this work. The SCD increases with higher capture rates, which is mainly due to increased cooling in the lean amine cooler, the load of which increases with higher capture rates because of increasing solvent circulation and the higher rich-solvent temperatures leaving the absorber (cf. temperature profiles in Figure 10). Higher rich-solvent temperatures cause higher lean-solvent temperatures leaving the cross-heat exchanger. It should be noted that the enthalpy of the absorber top gas decreases with increasing capture rates and that the cooling of incoming gas in the DCC is not included here (outside of scope; cf. Figure 2). The SPD (Figure 11b) decreases with higher capture rates, which is fundamentally caused by the constant load of the flue gas fan, which is forcing a constant flow of gas through the column, irrespective of the capture rate. Most pumps associated with circulating solvent increase slightly their demand in line with the increasing solvent circulation rate for higher capture rates. Cooling water pumps follow the trend of the SCD in the left panel. It should be noted that the power demand is 1–2 orders of magnitudes smaller than the energy requirements for solvent regeneration (reboiler) and process cooling. Note that CO_2 compression (e.g., to 15 barg for shipping) is not included here (CO_2 conditioning is outside of scope; cf. Figure 2).

4.2.2. Comparison of Off-Design Partial Capture with Intercooling. To quantify further the effect of the absorber temperature on the SRD, off-design partial capture is compared to intercooling on-design (95% capture). Figure 12 compares

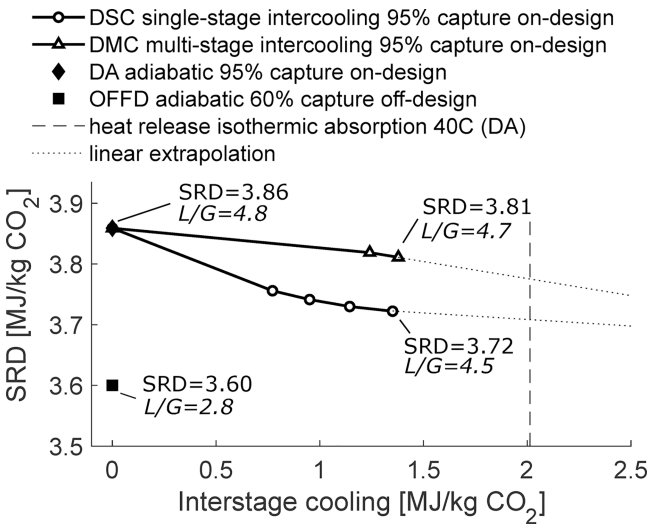

Figure 12. Comparison of the SRD and liquid-to-gas ratios for adiabatic (DA) and intercooled absorbers (DSC, DMC) in on-design mode, as compared to an adiabatic OFFD system operating close to the minimum SRD. The heat release of isothermic absorption at 40 °C, corresponding to the DA case, is shown to exemplify the extent of intercooling (DSC, DMC). Plots are obtained from the model simulations conducted in this work.

the SRD and L/G ratios for the four cases (cf. Section 3.2.3): adiabatic on-design (DA); single-stage intercooling on-design (DSC); multistage intercooling on-design (DMC); and adiabatic off-design partial capture (OFFD). Figure 12 demonstrates that intercooling on-design cannot achieve an SRD similar to that provided by the adiabatic off-design absorber, which captures less CO_2. This is indicated by the extrapolated slopes of the intercooling curves (DSC, DMC) which would not reach SRD values similar to OFFD even if the cooling was to reach a level similar to that linked to the heat

https://doi.org/10.1021/acs.iecr.2c02205
Ind. Eng. Chem. Res. 2022, 61, 14305–14323

release due to the isothermic reactions occurring in the absorber at 40 °C (absorber feed temperature). Although multistage cooling leads to a lower bulge temperature of 79 °C, as compared to single-stage cooling (84 °C), the single-stage intercooling at the bottom of the absorber leads to a lower SRD. The intercooling stage (DSC) that yields the lowest SRD (3.71 MJ/kg CO_2) was localized to the bottom-quarter of the column (between Stages 26 and 27 of 30), which is in accordance with the literature.[53,54] Cooling closer to the bulge location at the top of the column has a weaker effect on the bulge temperature (Figure S.7 in the Supporting Information), and the resulting rich solvent loading is only slightly increased compared to an adiabatic column (DA). As illustrated in Figure 13, the SRD

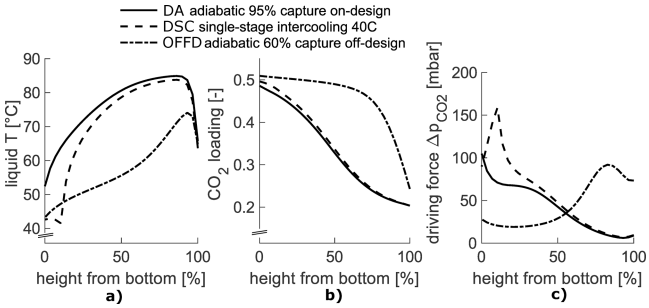

Figure 13. Modeled absorber profiles for liquid temperature (a), molar CO_2 loading (b), and difference in partial CO_2 pressure between the bulk gas phase and phase equilibrium (c) for an adiabatic on-design (DA), single-stage intercooling at 40 °C (DSC) and OFFD. Note that the ordinates in (a) and (b) are truncated. Plots are obtained from the model simulations conducted in this work.

reduction provided by single-stage intercooling (DSC) is mainly attributed to the provision of a cooler liquid phase at the bottom of the column (Figure 13a) away from the pinch, which enhances the driving forces (Figure 13c) and leads to increased loading at the bottom of the column (Figure 13b), as compared to DA, which captures the same amount of CO_2 (95%). The studied intercooling cases DSC and DMC also consistently showed up to 3 and 6% smaller column diameters, respectively. Thus, intercooling leads to more-compact equipment as well as lower SRD.

In Figure 13, the adiabatic partial capture absorber (OFFD) does not exhibit a lean-end pinch, and, thus, exhibits large driving forces and absorption at the top of the column (cf. Figure 10). Because less liquid is brought into the column (lower L/G), a larger share of the heat leaves with the gas, which is in line with the bulge theory of Kvamsdal and Rochelle. In addition, Figure 14 demonstrates that significantly less energy leaves the column via the liquid phase (~50%) in the off-design case than in the on-design case (~86%). Thus, both the overall lower liquid temperature and the reduced amount of liquid (lower L/G) in the OFFD case lead to a larger loading of CO_2, which results in a significantly lower SRD compared to intercooled absorbers (DSC) that operate on-design at higher L/G and capture more CO_2.

4.2.3. Partial Capture—Impacts of Column Design and CO_2 Concentration on Energy Performance. The following results of the design study (see Section 3.2.3) characterize the energy performance of off-design partial capture as a function of column design and CO_2 feed concentration. Ex ante, it should be mentioned that the design for 95% capture with the lowest SRD was found for lean loadings in the range of 0.18−0.20 mol CO_2/

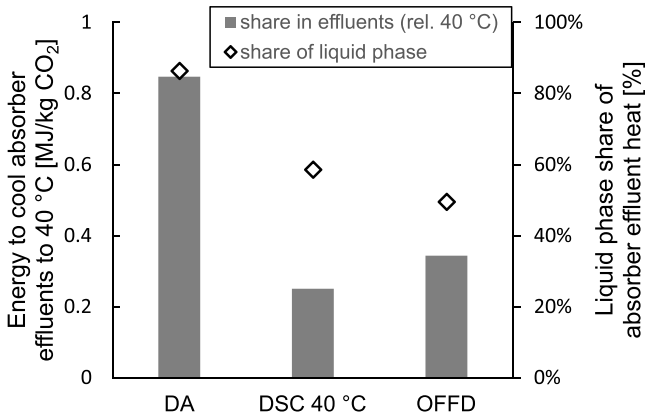

Figure 14. Energy levels required to cool the absorber effluents to the feed temperature (40 °C) and the shares of heat in the effluent liquid phase for the adiabatic on-design (DA), single-stage intercooling at 40 °C (DSC), and OFFD cases. Plots are obtained from the model simulations conducted in this work.

mol MEA (while performing u-curves) for the entire span of the varied parameters (CO_2 concentration, packing height, flooding approach).

The impacts of column design (absorber height, absorber, and stripper design factor) on the energy performance indicators of partial capture for a CO_2-rich gas (20 vol %) are illustrated in Figure 15. The following observations can be made:

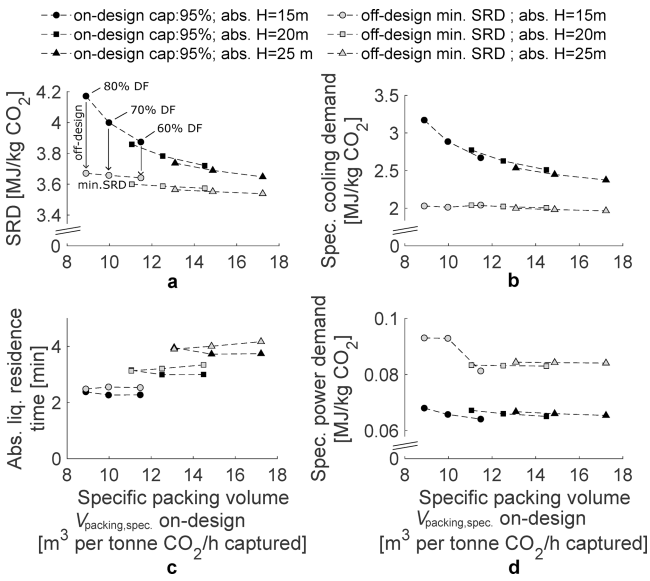

Figure 15. Impact of column design on off-design partial capture (minimized SRD) performance relative to 95% capture in on-design mode in terms of: SRD (a), SCD (b), absorber liquid residence time (c), and SPD (d), for a CO_2 concentration of 20 vol %. Plots are obtained from the model simulations performed in this work. Note that the abscissa denotes the specific packing volume $V_{packing,spec}$ as a sum of absorber and stripper packings and relates to the design point (95% capture). The design point varies as a combination of absorber height [abs. H; 15, 20, and 25 m] and design factor (DF; 60, 70, and 80%) in both columns. For each absorber height, three points corresponding to the design factor DF are plotted, as exemplified in panel (a). The off-design points represent the capture rate [50−60%] at which the minimum SRD was obtained for each respective design (same abscissa value). Note that the ordinates in plots a, b, and d are truncated.

https://doi.org/10.1021/acs.iecr.2c02205
Ind. Eng. Chem. Res. 2022, 61, 14305−14323

- The on-design (black symbols) SRD and SCD decrease with larger specific packing volumes (Figure 15a,b). The overall decreases throughout the entire span of packing volumes were 14 and 25%, for the SRD and specific cooling, respectively. This is as expected, because the absorber liquid residence time increases with the absorber height, as illustrated in Figure 15c.
- The minimum SRD achieved at off-design partial capture (gray symbols) follows a similar trend, although it is affected by the packing volume to a lesser extent—an approximate decrease of 4% throughout the studied span (Figure 15a). The off-design cooling demand is not affected by the column packing volume (Figure 15b).
- The difference between on-design and off-design with regard to the energy demand for solvent regeneration and cooling diminishes with a larger specific packing volume. This means that the levels of energy savings achievable through partial capture are fundamentally dependent upon the chosen design.
- Both the on-design and off-design SPDs (Figure 15d) are independent of the column design. An exception to this is the somewhat higher off-design power demand predicted for an absorber height of 15 m and design factors of 70 and 80%. This is likely coupled to a shift in the location of the minimum SRD from a capture rate of 60% (all other points) to 50%, which implies that less CO_2 is captured and, thus, there is a higher SPD (see Figure S.8 in the Supporting Information).
- The increase in the column diameter [corresponding to a decrease in the design factor/flood approach; see eq 3] at constant absorber height has effects on the SRD and the specific cooling that are similar to those seen for variations of the absorber packing height (Figure 15a,b). This is in line with the experimental findings of Mangalapally and Hasse,[33] who have described the impact of the gas factor on the SRD. For the power demand, a weak impact can also be observed (Figure 15d). This is likely linked to a decrease in the L/G with larger column diameters. It is worth pointing out that the absorber liquid residence time (and, thus, the liquid holdup implicitly) was less-affected by the column diameter than by the absorber packing height (Figure 15c).

The impact of feed CO_2 concentration on the off-design SRD curve is presented in Figure 16. A priori, a higher CO_2 concentration gives a lower SRD (Figure 16a). Noteworthy is the more-pronounced exponential increase in SRD above a capture rate of 90% for lower CO_2 concentrations (Figure 16b). The stronger exponential character is coupled to the relatively low driving force (low CO_2 partial pressure) when targeting high capture rates (cf. Figures S.5 and S.6 in the Supporting Information). These difficulties in reaching a low CO_2 partial pressure in the exiting gas for lower CO_2 concentrations at 95% capture lead to a higher potential for energy savings from off-design partial capture. Importantly, the deviations from the minimum SRD related to the design point (Figure 16c) were largest above 90% capture, showing 77 and 70% for 4 vol $\%_{wet}$ CO_2 and 10 vol $\%_{wet}$ CO_2, respectively. For 20 vol $\%_{wet}$ CO_2, however, almost half of the deviation (49%) occurred below 90% capture. This renders off-design partial capture especially promising for high CO_2 concentrations. Surprisingly, the SRD deviation for 20 vol $\%_{wet}$ CO_2 was higher than for 10 vol $\%_{wet}$ CO_2 between 60 and 90% capture (Figure 16b). This implies

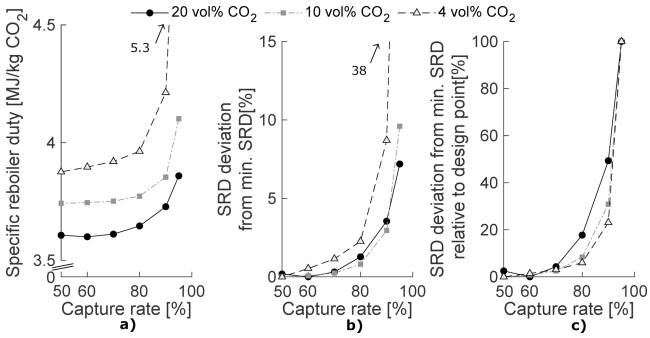

Figure 16. Impacts of CO_2 concentration on the off-design SRD curve (a), the deviation from minimum SRD (b), and the deviation from minimum SRD relative to the design point (c), for an absorber packing height of 20 m and design factor of 80%. Plots obtained from the model simulations performed in this work. Note that the ordinate in (a) is truncated.

that the SRD increases faster with the capture rate for 20 vol $\%_{wet}$ CO_2 than it does for 10 vol $\%_{wet}$ CO_2 despite the larger driving forces (cf. Figures 10 and S.6 in the Supporting Information). The likely reason for this is the larger exothermic reaction and temperature build-up in the absorber for 20 vol $\%_{wet}$ CO_2.

The results shown in Figure 17 demonstrate that the achievable energy savings for off-design partial capture are

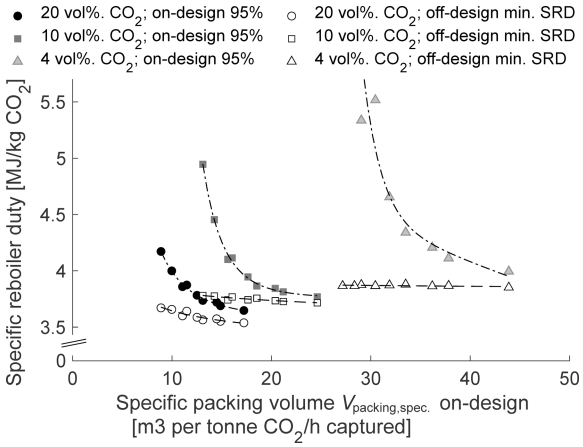

Figure 17. SRD for on-design (95% capture, filled icons) and off-design (minimum SRD, nonfilled icons) partial capture depending on the specific packing volume at the design point and the feed CO_2 concentration. Each off-design point corresponds to the on-design point at the same abscissa value. Note that the abscissa denotes the specific packing volume $V_{packing,spec}$ as a sum of absorber and stripper packings and relates to the design point (95% capture). Plots obtained from the model simulations performed in this work. Note that the ordinate is truncated.

fundamentally related to the decisions made regarding column design and the prevailing feed gas CO_2 concentration. The span of the energy savings, that is, the deviation of the design point SRD from the minimum SRD (difference between the filled and open symbols in Figure 17), becomes larger with decreasing CO_2 concentration, at 3−14%, 1−31%, and 4−78% for 20 vol $\%_{wet}$ CO_2, 10 vol $\%_{wet}$ CO_2, and 4 vol $\%_{wet}$ CO_2, respectively. Furthermore, it is apparent that higher CO_2 feed concentrations generally require a less-specific packing volume (abscissa value), which means smaller absorber columns, and that the off-design minimum SRD gradient becomes flatter for lower CO_2

https://doi.org/10.1021/acs.iecr.2c02205
Ind. Eng. Chem. Res. 2022, 61, 14305−14323

concentrations. For 4 vol $\%_{wet}$ CO_2, the gradient was close to zero. It should also be noted that the location of the minimum SRD was found at capture rates in the range of 50−70%. A larger packing volume seems to push the location of the minimum SRD to higher capture rates for 20 vol $\%_{wet}$ CO_2 and 10 vol $\%_{wet}$ CO_2, as indicated in Figure S.8 in the Supporting Information. Additional plots and derived functions for on/off-design energy demands and heat exchanger areas fitted to the model output are provided in Sections 2.5−2.9 in the Supporting Information.

5. DISCUSSION

The discussion is divided into three sections. In the first section, the experimental and modeling results are compared to each other regarding the absorber temperature, energy performance of partial capture, and column height. The second section describes the significance of the experimental campaign, while the third section discusses the implications of this work for the design of partial capture and its application in a stepwise CCS deployment with inherent full-capture-ready design.

5.1. Comparison of Experimental and Modeling Results. *5.1.1. Absorber Temperature Bulge.* The experimental and modeling results show good agreement concerning the bulge temperature's magnitude and location. The high CO_2 concentration in the SMR flue gas induces a bulge temperature as high as 85 °C (gases with lower CO_2 concentrations, e.g., the flue gas of a gas-fired CHP plant (4% CO_2), have bulge temperatures closer to 50 °C). For capture rates in the range of 90−95%, the model reveals that the bulge location coincides with the so-called "lean-end pinch" at the top of the column, which Kvamsdal and Rochelle[36] have described as "atypical". The colocation of the bulge and pinch may imply a hindered mass transfer, which would explain the dramatic increase in SRD observed above 90% capture. This seems especially relevant when high capture rates are targeted for gases with low partial pressures of CO_2.

5.1.2. Absorber Temperature Control. The experiment showed a decrease in SRD of ∼0.1 MJ/kg CO_2 when the ingoing gas temperature was cooled by 20°C. The modeled absorber intercooling decreased the SRD by 0.1−0.15 MJ/kg CO_2. However, a higher cooling demand is required for the intercooling ($L/G > 1$). The model results obtained here for 20 vol $\%_{wet}$ CO_2 indicate that intercooling at the bottom of a lean-end pinch column—where the rate of absorption is highest—yields SRD savings of 4%, as compared to the case with on-design capture of 95%. Rezazadeh et al. have shown similar total energy (pump work plus heat) savings related to the intercooling of gases at 4 vol % CO_2, albeit at lean loadings of >0.30, where the adiabatic column operates close to the critical L/G (bulge and pinch coincide in the middle of the column).[35] Such an operational regime was, however, not found in the present work, because the design points (u-curve minimization of SRD vs lean loading) were all found to be in the range of 0.18−0.20 mol CO_2/mol MEA. Other studies have shown that the energy savings achieved with intercooling diminish with decreasing CO_2 concentrations[40] and that intercooling has a limited effect when applied at lower CO_2 capture rates.[13] Overall, both the experiments and the modeling confirm that active management of the absorber temperature via intercooling or gas cooling can lead to considerable SRD savings for CO_2-rich gases. Furthermore, the model finds reduced column diameters (packing volume) for intercooling, as has also been described by Rezazadeh et al.[35] and Le Moullec et al.[55]

5.1.3. Energy Performance of Partial Capture. The measured drop in SRD with lower capture rates was greater than the drop predicted by the model (cf. Figure 9). Despite efforts to vary in a reasonable manner the model configurations (lean temperature, cross heat exchanger dT, reaction conditioning factor, interfacial area factor), the modeled result could not be brought closer (within a deviation of 5%) to the measured point of ∼3.4 MJ/kg at ∼60% capture. Possible reasons for this deviation are: (1) the spread in the experimental values (see Figure 6) and (2) differences between the actual MTU process design and the standard flowsheet modeled in Aspen Plus. It is noteworthy that the MTU was operated below its nominal gas capacity of 1000 Sm^3/h (see Table 3), indicative of a rather low-level flooding approach. The model results presented in Section 4.2.3 indicate lower off-design energy savings, for example, deviations from the minimum SRD, for a lower design factor (flooding approach). However, the experimental value at ∼60% capture implies a relatively large deviation of 8−11% from the minimum SRD, implying that the value is an outlier. Askestad et al.[30] have reported a deviation of 5−6% from the minimum SRD in the capture rate range of 70−90% measured with the MTU; however, the CO_2 concentration and the solvent used were not disclosed.

5.1.4. Variations of the Packing Height and Design Factor. The experimentally observed increase in SRD of ∼0.1 MJ/kg CO_2 when the packing height was reduced from 18 to 11 m (Figure 7) is comparable in magnitude to the modeled height reduction from 20 to 15 m (Figure 15) for design factors (flooding approach) of 70 and 60%. This implies that the flooding approach reached during the experiments was likely <60% (operation below the maximum gas capacity), which would compensate for the rather large drop in packing height of 7 m (38%). This is also supported by the relatively high specific packing volumes for the experiments with ∼19 and ∼24 m^3/t CO_2/h, for packing heights of 11 m and 18 m, respectively, which are higher than the values achieved in the on-design model (Figure 15). The low experimental flooding approach could may also explain the rather flat behavior of the u-curve (Figure 5) as compared to Gjernes et al.,[17] who reported a specific packing volume of 37 m^3/t CO_2/h for 4 vol $\%_{wet}$ CO_2 for the TCM plant, which is in better agreement with the modeled on-design values in the present study (30−44 m^3/t CO_2/h cf. Figure 17).

5.2. Significance of Experimental MEA Campaign at the Pilot Scale. The experimental findings for CO_2 capture from SMR flue gas with 18−20 vol % CO_2 using MEA complement the existing data in the literature linked to pilot runs with lower concentrations (4−15 vol $\%_{wet}$ CO_2) (cf. Table 1). The main differences that we observed were: (1) the temperature build-up in the absorber (see Figure 6 and the discussion above); (2) an SRD performance that is improved compared to gas-based and similar to coal-based flue gases (cf. Figure 5 and Table 1); and (3) indications of more-severe degradation. The latter phenomenon we associate with the temperature in the absorber, as evidenced by increased levels of organic degradation products and significantly higher emissions of ammonia (ppmv) in the absorber top gas. The higher ammonia emissions are likely caused by the higher temperature in the absorber, which is expected to: (1) improve the kinetics of the oxidative degradation pathways and (2) increase the release of volatile ammonia to the gas phase. However, it is unclear as to how much extra ammonia is released from the solvent entering the absorber with respect to the incoming gas, given that the $L/$

https://doi.org/10.1021/acs.iecr.2c02205
Ind. Eng. Chem. Res. 2022, 61, 14305−14323

G to is higher for high CO_2 concentrations than for low CO_2 concentrations. With respect to the stability of amine solvents, it is important to mention the performance of one of ACC's proprietary amine-based solvents, the S26, which, after over 3000 h capturing 90% CO_2 from the same gas (steam reformer flue gas), only shows a solvent loss of 0.11 kg/t CO_2 (1.1 kg/t CO_2 for MEA), ammonia emissions of only 1−2 ppm (20−100 ppm for MEA; cf. Figure 8), and no visible discoloring (for MEA cf. Figure S.2 in the Supporting Information). These and other details on the S26 campaign are given in the project report of Preem CCS.[37]

The experimental findings reported here confirm that the energy savings achieved through partial capture can be substantial, thereby verifying a previous assessment of the energy performance of partial capture in a study[13] that also examined the techno-economic aspects. Furthermore, the on-site pilot campaign demonstrates the technical feasibility of CO_2 capture from flue gases emitted from steam reformer furnaces operated with a pressure swing adsorption (PSA) off-gas, natural gas or butane, with capture rates of up to 95%. To the best of our knowledge, the MEA campaign of CO_2 capture from steam reformer flue gas presented here is one of the first to make the data publicly available for a pilot scale that is representative of a full-scale plant. Following its commercial application for hydrogen production,[56] CO_2 capture from a steam reformer syngas has been demonstrated in pioneering CCS projects on hydrogen production at: Port Arthur in the US;[57] Quest CCS in Canada;[58] and the Tomakomai Project (capture from PSA tail gas) in Japan.[59] Because capture from syngas will only capture ∼56% (at plant level), CO_2 capture from the steam reformer/autothermal reformer flue gas at capture rates >90% (at plant level) will be important for achieving low-carbon hydrogen production at emission levels similar to those seen for hydrogen production from electrolysis using >90% renewable energy.[60]

5.3. Implications for the Design of Partial Capture and Its Application in an Inherently Full-Capture-Ready CCS Rollout. The findings described in Section 4.2.3 indicate two distinct regimes in the curves for SRD versus capture rate (Figure 16). For capture rates >90%, the curves are characterized by the partial CO_2 pressure at the absorber top, as a function of the ingoing CO_2 concentration and the capture rate target. For capture rates <90%, the shape of the curve is affected by temperature levels as a function of the extent of the reaction and the L/G, both of which increase with larger changes in the CO_2 partial pressure, which means that they are higher for CO_2-rich gases at a given capture rate. Increases in the packing volume (absorber packing height, design factor) consistently led to flatter gradients at capture rates <90% and generally lower energy savings for off-design partial capture. This implies that off-design partial capture with capture rates of 50−90% is especially energy-efficient for high CO_2 concentrations. For low CO_2 concentrations, the energy savings accrued from reducing the capture rate to <90% are limited to cases where the design is determined by a high installation cost (small packing volume) rather than the energy cost. Furthermore, for high CO_2 concentrations, off-design partial capture could contribute to effective emission control, simply because the temperature levels are significantly lower in the absorber column. The extension to full capture could then be accompanied by intercooling, to help mitigate the high temperatures. However, it must be emphasized that other solvents could see less-dramatic temperature changes with changes in the capture rate.

Concerning the design point, the present numeric modeling assumes a capture rate of 95% instead of the historically assumed rate of 90%. This is motivated, for example by Danaci et al.,[61] by the small cost increase when raising the capture rate from 90 to 95%. Higher capture rates of ∼99% can also be targeted, implying larger increases in SRD and cost. The impacts of capture rates >90% on cost have been assessed in detail by Brandl et al.[62] and Feron et al.[63]

Regarding the heat supply to a full-scale implementation of CO_2 capture at the refinery test site, we refer to a site-specific assessment[11] that found that capture of 90% of CO_2 from the steam reformer flue gas could be powered by residual heat exclusively. For stand-alone "blue" hydrogen production (90% capture from SMR flue gas with MEA), an IEAGHG report[56] finds an increase in fuel consumption by ∼10% compared to a plant without CO_2 capture.

It should be noted that the minimum wetting rate for the structured packing was not exceeded in either the absorber or the stripper column in any of the model runs when reducing the capture rate. However, model runs at lower capture rates were associated with a risk of exceeding the minimum pressure drop in the stripper packing, with lower gas velocities at lower capture rates. This could be mitigated by appropriate selection of the packing or vertical subdivision of the packing. However, the successful pilot operation at capture rates as low as ∼60% indicates that this may not be a crucial factor.

We propose a concept whereby off-design partial capture is applied in a stepwise CCS deployment with inherent full-capture-ready design. Thus, in a first step, off-design partial capture could be implemented and operated at lower capture rates (50−70%). In a second implementation phase, CCS operations could be extended to full capture by adding heat exchange surfaces and by building additional CO_2 conditioning plants downstream of the CO_2 capture plant. Although immediate implementation of full capture could be more economic per ton of CO_2 and would mitigate more CO_2 accumulatively over the lifetime of the plant (as exemplified in[37]), we believe that the stepwise deployment of CCS (to reach full capture) based on off-design partial capture has advantages:

- For "early movers" who want to implement CCS but want to do so gradually, because: (1) partial capture will initially (first phase of implementation) require less capital in absolute terms and possibly also in terms of specific cost (€ per ton of CO_2)[13] and thus represent a lower risk than an immediate implementation of full capture and (2) carbon prices sufficient to trigger full capture might first be expected in the future.
- For plants that have constraints in relation to supplying the necessary energy, for example, the Norcem Brevik plant which has based its site-level capture rate of 50% on the available residual heat.[64] The potential energy savings per ton of CO_2 captured through off-design partial capture would allow maximization of the captured CO_2 during the first phase of implementation. Achieving full capture would, thereafter, require additional supplies of energy over time.
- For industries/waste-to-energy plants that want to operate with varying load initially, for example, due to seasonal variations with regard to heat availability (e.g., due to district heating), where the capture plant is designed for a peak heat load.[65,66]

https://doi.org/10.1021/acs.iecr.2c02205
Ind. Eng. Chem. Res. 2022, 61, 14305−14323

Partial capture can of course only be applied to fossil fuel-based emissions, as long as it is consistent with climate targets. To comply with these targets as formulated in the Paris Agreement, global carbon emissions must be net-zero by around year 2050. It should be noted that the modeling approach used in this work is focused on the absorber and stripper columns, while the remaining heat exchanger equipment was modeled in on-design mode intentionally. In the context of stepwise implementation of CCS via partial capture, partial capture with off-design columns and heat exchangers that are designed for the actual partial capture solvent circulation and CO_2 flow will initially be more-economic than overdesigning the heat exchangers (first implementation phase). This is because plate heat exchangers can be easily extended or added for full capture later on (second implementation phase), at a low additional cost compared to installing full-capture-sized equipment from the beginning (cost scaling exponent close to 1[11]). If sufficient CO_2 flows are present (e.g., ∼600 kt/a[37]), the cost of conditioning units scales approximately linearly as well.[37] Thus, the installation of two conditioning plants (one sized for partial capture, and an additional unit to reach full capture) instead of one may not imply a significant extra cost (apart from projecting two units instead of one). In particular, if the alternative is to operate the CO_2 compression in part-load mode, which may require the recirculation of CO_2 to prevent a surge,[37] this will significantly increase the specific power consumption per captured ton of CO_2 (15 barg compression requires ∼0.26 MJ/kg CO_2,[67] which would double to 0.52 MJ/kg CO_2 for a recirculation rate of 50%).

To develop this idea further, an economic analysis of a stepwise CCS implementation based on off-design partial capture is needed that goes beyond the scope of the previous work[13] and includes the pathway to full capture. The results of this work clearly indicate that the energy savings achievable via off-design partial capture are dependent upon the choice of column design. For stepwise implementation of CCS via partial capture, this means that the choice of the design point will need to take into account the techno-economic aspects of both on- and off-design operation of the columns and will likely depend on the time difference between the two implementations and on the underlying ratio of installation to energy costs. As a suggestion for future work, a net-present-value analysis could compare the stepwise implementation via partial capture with full-capture ready design to: (1) evaluate immediate full capture and (2) assess the alternative of building two separate capture plants, each designed to capture >90% of the ingoing CO_2. The functions for off-design energy requirements and heat exchanger areas appended in Sections 2.5−2.9 of the Supporting Information could be valuable inputs to such an analysis.

6. CONCLUSIONS

This work reports unique measurements of the CO_2 captured from a slipstream of steam reformer flue gas (18−20 vol $\%_{wet}$ CO_2) at the Preem refinery located on the west coast of Sweden. The campaign tested capture with 30 wt % aqueous MEA for ∼500 h in the MTU used by Aker Carbon Capture AS, at a scale (full column height; up to 200 kg CO_2/h) that is considered to be representative of a full-scale plant. A numerical model was constructed for comparison and interpretation of the measurement data and for a design study of partial capture from CO_2-rich flue gases.

The test campaign successfully demonstrates the technical feasibility of amine-based capture of up to 95% of the CO_2 from the steam reformer flue gas. The energy required for solvent regeneration, the SRD was measured as 3.6−3.8 MJ/kg CO_2 for ∼90% capture. Increased degradation of MEA (evidenced inter alia by increased emissions of ammonia) was observed, which we attribute to the high temperatures observed in the absorber (bulge temperatures of ∼85 °C). The tests, which included variation of key process parameters, revealed moderate energy savings (SRD) of 2−3% both for flue gas cooling (decrease from 50 to 30 °C) and for increased absorber packing height (from 11 to 18 m). More significant energy savings (SRD) of 7−10% were assessed when the capture rate was reduced from ∼90 to ∼60%, verifying the substantial energy savings potential of partial capture operating in off-design mode.

The modeling work reveals that partial capture in off-design mode (∼60% capture) leads to an absorber operation that is characterized by a rich-end pinch and a bulge temperature of lesser magnitude (∼73 °C) located slightly more toward the top than is the case for on-design full capture of 95% of the CO_2. This, in combination with the lower L/G ratios for partial capture, leads to a higher rich loading of the solvent, ultimately resulting in a lower SRD. The achievable SRD savings with partial capture (on-design SRD values at 95% capture deviated by 1−78% from the minimum SRDs at 50−70% capture) were shown to be ultimately a function of the column geometry (absorber packing height and design factor, that is, approach to flooding) and the CO_2 feed concentration. Thus, it is concluded that: (1) the SRD savings decrease when the columns are designed to have larger specific packing volumes (greater absorber height, lower design factors/approach to flooding) and (2) the share of SRD savings that manifests below 90% capture increases with increasing CO_2 concentration (coupled to higher absorber temperatures), making off-design partial capture especially interesting for large point sources with high CO_2 concentrations.

In addition to the experimental verification, this work maps the fundamental characteristics of off-design partial capture and introduces the concept of stepwise CCS implementation based on partial capture that is designed to be inherently full-capture ready.

■ ASSOCIATED CONTENT

Supporting Information

The Supporting Information is available free of charge at https://pubs.acs.org/doi/10.1021/acs.iecr.2c02205.

Experimental data from the MEA campaign (Section 1) and additional modeling results and regressed functions based on the model output (Section 2) (PDF)

■ AUTHOR INFORMATION

Corresponding Author

M. Biermann − *Division of Energy Technology, Chalmers University of Technology, SE-41296 Gothenburg, Sweden;* orcid.org/0000-0001-8731-267X; Email: max.biermann@chalmers.se

Authors

F. Normann − *Division of Energy Technology, Chalmers University of Technology, SE-41296 Gothenburg, Sweden*

F. Johnsson − *Division of Energy Technology, Chalmers University of Technology, SE-41296 Gothenburg, Sweden*

R. Hoballah − *Aker Carbon Capture Norway AS, NO-1325 Lysaker, Norway*

https://doi.org/10.1021/acs.iecr.2c02205
Ind. Eng. Chem. Res. 2022, 61, 14305−14323

K. Onarheim − *Aker Carbon Capture Norway AS, NO-1325 Lysaker, Norway*

Complete contact information is available at: https://pubs.acs.org/10.1021/acs.iecr.2c02205

Notes

The authors declare no competing financial interest.

■ ACKNOWLEDGMENTS

The authors thank the partners involved in the Preem CCS project for good collaborations. Special thanks to the staff at Aker Carbon Capture AS for the planning, conduction, and data evaluation of the test campaign, and the staff at the Preem refinery in Lysekil for their support and assistance during and in preparation for the campaign.

■ NOTATION

d	calculated column diameter (m)
$\mathrm{Dev}_{\mathrm{SRD}}$	deviation from minimum SRD (%)
$\mathrm{Dev}_{\mathrm{SRD,\ rel.\ design}}$	deviation from minimum SRD relative to the SRD at the design point (%)
DF	design factor; relates operating gas capacity factor to gas capacity at flooding (%)
F	gas capacity factor (at design stage) ($\sqrt{\mathrm{Pa}}$)
h	packing height (structured packing) (m)
$\dot{m}_{\mathrm{CO_2,\ captured}}$	mass flow of captured CO_2 (kg/s or t/h)
P_{rotary}	electric power consumption for rotary equipment, such as flue gas fan, solvent pumping, cooling water pumping and auxiliary pumps (make-up, column reflux etc.) (MW)
$\dot{Q}_{\mathrm{cool}}$	process cooling for the units: lean amine cooler, stripper top condenser, and CO_2-depleted gas cooler (∼washer) (MW)
$\dot{Q}_{\mathrm{reb}}$	reboiler duty (MW)
SRD	specific reboiler duty; experimental values reflect heat loss (MJ/kg CO_2)
$\mathrm{SRD}_{\mathrm{min}}$	minimum specific reboiler duty observed when varying the capture rate (MJ/kg CO_2)
$\mathrm{SRD}_{\mathrm{design,95\%}}$	specific reboiler duty at the design point (95% capture at a given column design) (MJ/kg CO_2)
SCD	specific cooling demand (MJ/kg CO_2)
SPD	specific power demand (MJ/kg CO_2)
$\tau_{\mathrm{liq,\ abs}}$	absorber liquid residence time; derived from calculated liquid holdup and lean solvent flow entering the absorber (min)
$u_{\mathrm{gas,\ design\ stage}}$	gas/vapor velocity at design stage (m/s)
$\rho_{\mathrm{gas,\ design\ stage}}$	gas/vapor density at design stage (kg/m^3)
$\dot{m}_{\mathrm{gas,\ design\ stage}}$	gas capacity at design stage (kg/s)
V_{holdup}	liquid holdup in the absorber packing (m^3)
$V_{\mathrm{packing,\ abs}}$	absorber packing volume (assuming cylindrical geometry) (m^3)
$V_{\mathrm{packing,\ str}}$	stripper packing volume (assuming cylindrical geometry) (m^3)
$\dot{V}_{\mathrm{lean\ solv,\ abs}}$	volume flow of lean solvent entering the absorber (m^3/min)

■ REFERENCES

(1) Hildebrand, A. N.; Herzog, H. J. Optimization of Carbon Capture Percentage for Technical and Economic Impact of Near-Term CCS Implementation at Coal-Fired Power Plants. *Energy Procedia* **2009**, *1*, 4135−4142.

(2) Singh, S.; Lu, H.; Cui, Q.; Li, C.; Zhao, X.; Xu, W.; Ku, A. Y. China Baseline Coal-Fired Power Plant with Post-Combustion CO_2 Capture: 2. Techno-Economics. *Int. J. Greenhouse Gas Control* **2018**, *78*, 429−436.

(3) IEA Greenhouse Gas R&D Programme (IEAGHG). Partial Capture of CO_2. 2009/TR2 2009.

(4) Schnellmann, M. A.; Chyong, C. K.; Reiner, D. M.; Scott, S. A. Deploying Gas Power with CCS: The Role of Operational Flexibility, Merit Order and the Future Energy System. *Int. J. Greenhouse Gas Control* **2019**, *91*, No. 102838.

(5) Roussanaly, S.; Vitvarova, M.; Anantharaman, R.; Berstad, D.; Hagen, B.; Jakobsen, J.; Novotny, V.; Skaugen, G. Techno-Economic Comparison of Three Technologies for Pre-Combustion CO_2 Capture from a Lignite-Fired IGCC. *Front. Chem. Sci. Eng.* **2020**, *14*, 436−452.

(6) Rezvani, S.; McIlveen-Wright, D.; Huang, Y.; Dave, A.; Mondol, J. D.; Hewitt, N. Comparative Analysis of Energy Storage Options in Connection with Coal Fired Integrated Gasification Combined Cycles for an Optimised Part Load Operation. *Fuel* **2012**, *101*, 154−160.

(7) Gardarsdottir, S. O.; Normann, F.; Andersson, K.; Johnsson, F. Process Evaluation of CO_2 Capture in Three Industrial Case Studies. *Energy Procedia* **2014**, *63*, 6565−6575.

(8) Normann, F.; Skagestad, R.; Biermann, M.; Wolf, J.; Mathisen, A. *CO2stCap-Reducing the Cost of Carbon Capture in Process Industry*. Final report; Chalmers University of Technology, 2019, https://research.chalmers.se/publication/512527.

(9) Biermann, M.; Ali, H.; Sundqvist, M.; Larsson, M.; Normann, F.; Johnsson, F. Excess Heat-Driven Carbon Capture at an Integrated Steel Mill − Considerations for Capture Cost Optimization. *Int. J. Greenhouse Gas Control* **2019**, *91*, No. 102833.

(10) Johnsson, F.; Normann, F.; Svensson, E. Marginal Abatement Cost Curve of Industrial CO_2 Capture and Storage − A Swedish Case Study. *Front. Energy Res.* **2020**, *8*, 1−12.

(11) Biermann, M.; Langner, C.; Roussanaly, S.; Normann, F.; Harvey, S. The Role of Energy Supply in Abatement Cost Curves for CO_2 Capture from Process Industry − A Case Study of a Swedish Refinery. *Appl. Energy* **2022**, *319*, No. 119273.

(12) Bains, P.; Psarras, P.; Wilcox, J. CO_2 Capture from the Industry Sector. *Prog. Energy Combust. Sci.* **2017**, *63*, 146−172.

(13) Biermann, M.; Normann, F.; Johnsson, F.; Skagestad, R. Partial Carbon Capture by Absorption Cycle for Reduced Specific Capture Cost. *Ind. Eng. Chem. Res.* **2018**, *57*, 15411−15422.

(14) NCCC; Southern Company; *The National Carbon Capture Center at the Power Systems Development Facility - Final report 2008−2014*; Southern Company Services Incorporated: Wilsonville, AL, 2014 https://doi.org/10.2172/1234431.

(15) Kwak, N.-S.; Lee, J. H.; Lee, I. Y.; Jang, K. R.; Shim, J.-G. A Study of the CO_2 Capture Pilot Plant by Amine Absorption. *Energy* **2012**, *47*, 41−46.

(16) Gorset, O.; Knudsen, J. N.; Bade, O. M.; Askestad, I. Results from Testing of Aker Solutions Advanced Amine Solvents at CO_2Technology Centre Mongstad. *Energy Procedia* **2014**, *63*, 6267−6280.

(17) Gjernes, E.; Pedersen, S.; Jain, D.; Åsen, K. I.; Hvidsten, O. A.; De Koeijer, G.; Faramarzi, L.; de Cazenove, T. *Documenting Modes of Operation with Cost Saving Potential at the Technology Centre Mongstad*; 14th Greenhouse Gas Control Technologies Conference Melbourne 21-26 October 2018 (GHGT-14); SSRN, 2019, DOI: 10.2139/ssrn.3366235.

(18) Gjernes, E.; Pedersen, S.; Cents, T.; Watson, G.; Fostås, B. F.; Shah, M. I.; Lombardo, G.; Desvignes, C.; Flø, N. E.; Morken, A. K.; De Cazenove, T.; Faramarzi, L.; Hamborg, E. S. Results from 30 wt% MEA Performance Testing at the CO_2Technology Centre Mongstad. *Energy Procedia* **2017**, *114*, 1146−1157.

(19) Faramarzi, L.; Thimsen, D.; Hume, S.; Maxon, A.; Watson, G.; Pedersen, S.; Gjernes, E.; Fostås, B. F.; Lombardo, G.; Cents, T.; Morken, A. K.; Shah, M. I.; De Cazenove, T.; Hamborg, E. S. Results from MEA Testing at the CO_2 Technology Centre Mongstad: Verification of Baseline Results in 2015. *Energy Procedia* **2017**, *114*, 1128−1145.

(20) Kvamsdal, H. M.; Haugen, G.; Svendsen, H. F.; Tobiesen, A.; Mangalapally, H.; Hartono, A.; Mejdell, T. Modelling and Simulation of the Esbjerg Pilot Plant Using the Cesar 1 Solvent. *Energy Procedia* **2011**, *4*, 1644−1651.
(21) Stec, M.; Tatarczuk, A.; Więcław-Solny, L.; Krótki, A.; Spietz, T.; Wilk, A.; Śpiewak, D. Demonstration of a Post-Combustion Carbon Capture Pilot Plant Using Amine-Based Solvents at the Łaziska Power Plant in Poland. *Clean Technol. Environ. Policy* **2016**, *18*, 151−160.
(22) Cousins, A.; Cottrell, A.; Lawson, A.; Huang, S.; Feron, P. H. M. Model Verification and Evaluation of the Rich-Split Process Modification at an Australian-Based Post Combustion CO_2 Capture Pilot Plant. *Greenh. Gases Sci. Technol.* **2012**, *2*, 329−345.
(23) Lemaire, E.; Bouillon, P. A.; Lettat, K. Development of HiCapt +TM Process for CO_2 Capture from Lab to Industrial Pilot Plant. *Oil Gas Sci. Technol.* **2014**, *69*, 1069−1080.
(24) Mangiaracina, A.; Zangrilli, L.; Robinson, L.; Kvamsdal, H. M.; Van Os, P. OCTAVIUS: Evaluation of Flexibility and Operability of Amine Based Post Combustion CO_2 Capture at the Brindisi Pilot Plant. *Energy Procedia* **2014**, *63*, 1617−1636.
(25) Knudsen, J. N.; Jensen, J. N.; Vilhelmsen, P. J.; Biede, O. Experience with CO_2 Capture from Coal Flue Gas in Pilot-Scale: Testing of Different Amine Solvents. *Energy Procedia* **2009**, *1*, 783−790.
(26) Knudsen, J. N.; Bade, O. M.; Anheden, M.; Bjorklund, R.; Gorset, O.; Woodhouse, S. Novel Concept for Emission Control in Post Combustion Capture. *Energy Procedia* **2013**, *37*, 1804−1813.
(27) Moser, P.; Schmidt, S.; Sieder, G.; Garcia, H.; Stoffregen, T. Performance of MEA in a Long-Term Test at the Post-Combustion Capture Pilot Plant in Niederaussem. *Int. J. Greenhouse Gas Control* **2011**, *5*, 620−627.
(28) Hamborg, E. S.; Smith, V.; Cents, T.; Brigman, N.; Pedersen, O. F.; De Cazenove, T.; Chhaganlal, M.; Feste, J. K.; Ullestad, Ø.; Ulvatn, H.; Gorset, O.; Askestad, I.; Gram, L. K.; Fostås, B. F.; Shah, M. I.; Maxson, A.; Thimsen, D. Results from MEA Testing at the CO_2 Technology Centre Mongstad. Part II: Verification of Baseline Results. *Energy Procedia* **2014**, *63*, 5994−6011.
(29) Knudsen, J. N.; Bade, O. M.; Askestad, I.; Gorset, O.; Mejdell, T. Pilot Plant Demonstration of CO_2 Capture from Cement Plant with Advanced Amine Technology. *Energy Procedia* **2014**, *63*, 6464−6475.
(30) Askestad, I.; Arne, K.; Bade, O. M.; Onarheim, K.; Lie, K. O.; Gorset, O.; Wanderley, R. R.; Knudsen, J. N.; Andersson, V. *Towards Full-Scale Carbon Capture − Results from the Mobile Test Unit in Various Industry Sectors*; Proceedings of the 15th Greenhouse Gas Control Technologies Conference; SSRN, 2021; pp 1−8.
(31) Tait, P.; Buschle, B.; Milkowski, K.; Akram, M.; Pourkashanian, M.; Lucquiaud, M. Flexible Operation of Post-Combustion CO_2 Capture at Pilot Scale with Demonstration of Capture-Efficiency Control Using Online Solvent Measurements. *Int. J. Greenhouse Gas Control* **2018**, *71*, 253−277.
(32) Bui, M.; Tait, P.; Lucquiaud, M.; Mac Dowell, N. Dynamic Operation and Modelling of Amine-Based CO_2 Capture at Pilot Scale. *Int. J. Greenhouse Gas Control* **2018**, *79*, 134−153.
(33) Mangalapally, H. P.; Hasse, H. Pilot Plant Study of Post-Combustion Carbon Dioxide Capture by Reactive Absorption: Methodology, Comparison of Different Structured Packings, and Comprehensive Results for Monoethanolamine. *Chem. Eng. Res. Des.* **2011**, *89*, 1216−1228.
(34) Shah, M. I.; Lombardo, G.; Fostås, B.; Benquet, C.; Kolstad Morken, A.; de Cazenove, T. *CO2 Capture from RFCC Flue Gas with 30w% MEA at Technology Centre Mongstad, Process Optimization and Performance Comparison*; 14th Greenhouse Gas Control Technologies Conference Melbourne; SSRN, 2019, DOI: 10.2139/ssrn.3366149.
(35) Rezazadeh, F.; Gale, W. F.; Rochelle, G. T.; Sachde, D. Effectiveness of Absorber Intercooling for CO_2 Absorption from Natural Gas Fired Flue Gases Using Monoethanolamine Solvent. *Int. J. Greenhouse Gas Control* **2017**, *58*, 246−255.
(36) Kvamsdal, H. M.; Rochelle, G. T. Effects of the Temperature Bulge in CO_2 Absorption from Flue Gas by Aqueous Monoethanolamine. *Ind. Eng. Chem. Res.* **2008**, *47*, 867−875.
(37) Biermann, M.; Harvey, S.; Kjärstad, J.; Anantharaman, R.; Fu, C.; Jordal, K.; Reyes Lúa, A.; Roussanaly, S.; Lundqvist, K.; Gorset, O.; Hoballah, R.; Wanderley, R.; Eikenes Seglem, H. *Preem CCS - Synthesis of Main Project Findings and Insights*; Chalmers University of Technology: Gothenburg, 2022.
(38) Aker Carbon Capture AS. Just Test - A complete carbon capture plant, mobile and modular (homepage of ACC) https://akercarboncapture.com/offerings/just-test/ (accessed August 15, 2022).
(39) Bade, O. M.; Knudsen, J. N.; Gorset, O.; Askestad, I. Controlling Amine Mist Formation in 2 Capture from Residual Catalytic Cracker (RCC) Flue Gas. *Energy Procedia* **2014**, *63*, 884−892.
(40) Garðarsdóttir, S. Ó.; Normann, F.; Andersson, K.; Johnsson, F. Postcombustion CO_2 Capture Using Monoethanolamine and Ammonia Solvents: The Influence of CO_2 Concentration on Technical Performance. *Ind. Eng. Chem. Res.* **2015**, *54*, 681−690.
(41) AspenTech. ENRTL-RK Rate-Based Model of the CO_2 Capture Process by MEA Using Aspen Plus - Version 10.0. 2017.
(42) Bravo, J. L.; Rocha, J. A.; Fair, J. R. Mass Transfer in Gauze Packings. *Hydrocarbon Process.* **1985**, *64*, 91−95.
(43) Stichlmair, J.; Bravo, J. L.; Fair, J. R. General Model for Prediction of Pressure Drop and Capacity of Countercurrent Gas/Liquid Packed Columns. *Gas Sep. Purif.* **1989**, *3*, 19−28.
(44) Chilton, T. H.; Colburn, A. P. Mass Transfer (Absorption) Coefficients Prediction from Data on Heat Transfer and Fluid Friction. *Ind. Eng. Chem.* **1934**, *26*, 1183−1187.
(45) Zhang, Y.; Chen, C. C. Modeling CO_2 Absorption and Desorption by Aqueous Monoethanolamine Solution with Aspen Rate-Based Model. *Energy Procedia* **2013**, *37*, 1584−1596.
(46) Pinsent, B. R. W.; Pearson, L.; Roughton, F. J. W. The Kinetics of Combination of Carbon Dioxide with Hydroxide Ions. *Trans. Faraday Soc.* **1956**, *52*, 1512−1520.
(47) Hikita, H.; Asai, S.; Ishikawa, H.; Honda, M. The Kinetics of Reactions of Carbon Dioxide with Monoethanolamine, Diethanolamine and Triethanolamine by a Rapid Mixing Method. *Chem. Eng. J.* **1977**, *13*, 7−12.
(48) Mackowiak, J. *Fluid Dynamics of Packed Columns*; Springer, 2010.
(49) Zhang, Y.; Chen, H.; Chen, C.-C.; Plaza, J. M.; Dugas, R.; Rochelle, G. T. Rate-Based Process Modeling Study of CO_2 Capture with Aqueous Monoethanolamine Solution. *Ind. Eng. Chem. Res.* **2009**, *48*, 9233−9246.
(50) SeperationTechnology.com. Packing Hydraulics Calculations http://seperationtechnology.com/packing-hydraulics/ (accessed January 3, 2022).
(51) Green, D. W.; Perry, R. H. *Perry's Chemical Engineers' Handbook*, 8th ed.; McGraw-Hill, 2007.
(52) Kolstad Morken, A.; Pedersen, S.; Romslo, E. Degradation and Emission Results of Amine Plant Operations from MEA Testing at the CO_2 Technology Centre Mongstad. *Energy Procedia* **2017**, *114*, 1245−1262.
(53) Cousins, A.; Wardhaugh, L. T.; Feron, P. H. M. Preliminary Analysis of Process Flow Sheet Modifications for Energy Efficient CO_2 Capture from Flue Gases Using Chemical Absorption. *Chem. Eng. Res. Des.* **2011**, *89*, 1237−1251.
(54) Sharma, M.; Qadir, A.; Khalilpour, R.; Abbas, A. Modeling and Analysis of Process Configurations for Solvent-Based Post-Combustion Carbon Capture. *Asia-Pac. J. Chem. Eng.* **2015**, *10*, 764−780.
(55) Le Moullec, Y.; Neveux, T.; Al Azki, A.; Chikukwa, A.; Hoff, K. A. Process Modifications for Solvent-Based Post-Combustion CO_2 Capture. *Int. J. Greenhouse Gas Control* **2014**, *31*, 96−112.
(56) IEAGHG; Techno - Economic Evaluation of SMR Based Standalone (Merchant) Hydrogen Plant with CCS; *Tech. Rev. 2017-02* **2017**, *TR 2017-02* (February), 286.
(57) Power, G.; Busse, A.; MacMurray, J. *Demonstration of Carbon Capture and Sequestration of Steam Methane Reforming Process Gas Used for Large-Scale Hydrogen Production*; Air Products and Chemicals, Inc.: Allentown, PA, 2018, DOI: 10.2172/1437618.
(58) Rock, L.; O'Brien, S.; Tessarolo, S.; Duer, J.; Bacci, V. O.; Hirst, B.; Randell, D.; Helmy, M.; Blackmore, J.; Duong, C.; Halladay, A.;

Smith, N.; Dixit, T.; Kassam, S.; Yaychuk, M. The Quest CCS Project: 1st Year Review Post Start of Injection. *Energy Procedia* **2017**, *114*, 5320−5328.
(59) Sawada, Y.; Tanaka, J.; Suzuki, C.; Tanase, D.; Tanaka, Y. Tomakomai CCS Demonstration Project of Japan, CO_2 Injection in Progress. *Energy Procedia* **2018**, *154*, 3−8.
(60) Ueckerdt, F.; Verpoort, P. C.; Anantharaman, R.; Bauer, C.; Beck, F.; Longden, T.; Roussanaly, S. *On the Cost Competitiveness of Blue and Green Hydrogen*; [Preprint], 2022, DOI: 10.21203/rs.3.rs-1436022/v1.
(61) Danaci, D.; Bui, M.; Petit, C.; Mac Dowell, N. En Route to Zero Emissions for Power and Industry with Amine-Based Post-Combustion Capture. *Environ. Sci. Technol.* **2021**, *55*, 10619−10632.
(62) Brandl, P.; Bui, M.; Hallett, J. P.; Mac Dowell, N. Beyond 90% Capture: Possible, but at What Cost? *Int. J. Greenhouse Gas Control* **2021**, *105*, No. 103239.
(63) Feron, P.; Cousins, A.; Jiang, K.; Zhai, R.; Shwe Hla, S.; Thiruvenkatachari, R.; Burnard, K. Towards Zero Emissions from Fossil Fuel Power Stations. *Int. J. Greenhouse Gas Control* **2019**, *87*, 188−202.
(64) Norcem; Heidelberg Cement Group. Norwegian CCS Demonstration Project - Norcem FEED - Redacted version of FEED Study (DG3) Report https://ccsnorway.com/wp-content/uploads/sites/6/2020/07/NC03-NOCE-A-RA-0009-Redacted-FEED-Study-DG3-Report-Rev01-1.pdf.
(65) Martinez Castilla, G.; Biermann, M.; Montañés, R. M.; Normann, F.; Johnsson, F. Integrating Carbon Capture into an Industrial Combined-Heat-and-Power Plant: Performance with Hourly and Seasonal Load Changes. *Int. J. Greenhouse Gas Control* **2019**, *82*, 192−203.
(66) Eliasson, Å.; Fahrman, E.; Biermann, M.; Normann, F.; Harvey, S. Efficient Heat Integration of Industrial CO_2 Capture and District Heating Supply. *Int. J. Greenhouse Gas Control* **2022**, *118*, No. 103689.
(67) Deng, H.; Roussanaly, S.; Skaugen, G. Techno-Economic Analyses of CO_2 Liquefaction: Impact of Product Pressure and Impurities. *Int. J. Refrig.* **2019**, *103*, 301−315.